

Perturbative QCD contribution to transverse single spin asymmetries in the Drell-Yan process and SIDIS

Sanjin Benić,¹ Yoshitaka Hatta^{2,3}, Abhiram Kaushik,⁴ and Hsiang-nan Li⁵

¹*Department of Physics, Faculty of Science, University of Zagreb, Bijenička c. 32, 10000 Zagreb, Croatia*

²*Physics Department, Brookhaven National Laboratory, Upton, New York 11973, USA*

³*RIKEN BNL Research Center, Brookhaven National Laboratory, Upton, New York 11973, USA*

⁴*Centre for Informatics and Computing, Rudjer Bošković Institute, HR-10002 Zagreb, Croatia*

⁵*Institute of Physics, Academia Sinica, Taipei, Taiwan 11529, Republic of China*



(Received 14 February 2024; accepted 6 April 2024; published 30 April 2024)

In a previous publication [Benić *et al.*, *Phys. Rev. D* **104**, 094027 (2021)], we have computed the perturbative QCD contribution to transverse single spin asymmetries (SSAs) in semi-inclusive deep inelastic scattering (SIDIS) involving the $g_T(x)$ distribution. In this paper, we first present a more efficient derivation of the asymmetries which is applicable to both transverse and longitudinal SSAs and correct some inconsistencies in our previous calculation. We then adapt the method to compute transverse SSAs in the Drell-Yan process proportional to $g_T(x)$ and its gluonic counterpart and discuss the crossing symmetry between the results for SIDIS and the Drell-Yan process. Finally, we present numerical results for various asymmetries measurable at the EIC, RHIC, COMPASS, and Fermilab (SpinQuest), including also part of the genuine twist-three corrections to $g_T(x)$ from a recent global analysis. We find that the asymmetries can reach percent-level magnitude, if the kinematics predominantly probes the large- x (valence) region of the polarized proton, but remain at subpercent levels otherwise.

DOI: [10.1103/PhysRevD.109.074038](https://doi.org/10.1103/PhysRevD.109.074038)

I. INTRODUCTION

In recent years, there has been renewed interest in the perturbative QCD contribution to single spin asymmetries (SSAs) [1–4] motivated by the ongoing and future experiments capable of the precision measurement of spin asymmetries up to high transverse momenta. By perturbative, we mean that the imaginary phase necessary to generate asymmetries comes from $2 \rightarrow 2$ hard (partonic) scattering kernels. For transverse single spin asymmetries (SSAs) A_{UT} , such a contribution was studied long ago [5,6] and had been largely neglected by the community owing to the purported proportionality to a current quark mass $A_{UT} \propto \alpha_s m_q$. On the other hand, longitudinal SSAs A_{UL} are insensitive to the mass effect and have been calculated within the standard collinear factorization framework in both the Drell-Yan [7,8] process and semi-inclusive deep inelastic scattering (SIDIS) [3].

In our previous publications [1,2], we have systematically extended the investigation of transverse SSAs in SIDIS to a subleading level. In the k_T -factorization framework, we

have identified the complete set of SSA sources up to two loops in hard kernels and to twist three in two-parton transverse-momentum-dependent (TMD) parton distribution functions (PDFs). We then focused on the asymmetries originating from the polarized quark distribution function $g_T(x)$, as well as its gluonic counterpart $\mathcal{G}_{3T}(x)$, which survives in the collinear factorization framework. The corresponding quark- and gluon-initiated $\mathcal{O}(\alpha_s^2)$ hard kernels for SIDIS were computed, and the resultant asymmetries A_{UT} associated with, e.g., the $\sin(\phi_h - \phi_S)$, $\sin \phi_S$, and $\sin(2\phi_h - \phi_S)$ harmonics, were predicted for measurements at the future Electron-Ion Collider (EIC). We have shown that in SIDIS, the naive relation $A_{UT} \propto m_q$ is incorrect and should be replaced by $A_{UT} \propto M_N$, where M_N is the proton mass. We have further performed a numerical analysis and found that some of the asymmetries could reach a percent level, manifesting the importance of high-accuracy studies in the considered kinematic regions.

In this paper, we first present, in Secs. II and III, a more efficient derivation of the asymmetries in SIDIS, which allows for a unified treatment of transverse and longitudinal SSAs. We take this opportunity to correct some inconsistencies in our previous results [2]. In Sec. IV, the formalism is extended to compute, for the first time, the contributions to transverse SSAs in the Drell-Yan process proportional to g_T and \mathcal{G}_{3T} in the $q\bar{q}$ annihilation and Compton scattering channels. Here, too, the approach is

Published by the American Physical Society under the terms of the [Creative Commons Attribution 4.0 International license](https://creativecommons.org/licenses/by/4.0/). Further distribution of this work must maintain attribution to the author(s) and the published article's title, journal citation, and DOI. Funded by SCOAP³.

applicable to longitudinal SSAs, and we reproduce the known results in the literature [7,8] for completeness. We then discuss how the formulas for SIDIS and the Drell-Yan process may be related by crossing symmetry. Finally in Sec. V, we numerically evaluate the various asymmetries. We update our predictions for the EIC and provide new predictions for the kinematics of the RHIC, COMPASS, and the Fermilab SpinQuest experiments. The possible impact of the genuine twist-three effects in light of the recent extraction of g_T [9,10] is also explored.

II. SSA IN SIDIS, QUARK-INITIATED CHANNEL

In this and the next sections, we revisit our calculation of SSAs in SIDIS in [2]. After reviewing the basic kinematics of the reaction and our new approach developed in [1,2], we propose a simpler derivation which helps reveal the inconsistencies in the previous analysis. It also facilitates the comparison with relevant results in the literature and allows a straightforward extension to the Drell-Yan case to be discussed in a later section.

A. Setup

Consider SIDIS in the so-called hadron frame where the virtual photon with the virtuality $q^2 = -Q^2$ and the transversely polarized proton with the momentum P^μ are collinear. We neglect the proton mass M_N whenever possible, so $P^\mu \approx \delta_+^\mu P^+$ is effectively a lightlike vector. We also need another lightlike vector $n^\mu = \delta^\mu_- / P^+$, such that $P \cdot n = 1$. The spin-dependent part of the cross section can be written as

$$\frac{d\Delta\sigma}{dx_B dQ^2 dz_f dq_T^2 d\phi d\chi} = \frac{\alpha_{em}^2 z_f}{128\pi^4 x_B^2 S_{ep}^2 Q^2} \times \sum_a \int \frac{dz}{z^2} D_1^a(z) L^{\mu\nu} w_{\mu\nu}^a, \quad (1)$$

where $x_B = Q^2 / (2P \cdot q)$ is the Bjorken variable, and $S_{ep} = (P + l)^2$ is the ep center-of-mass energy. μ and ν are the polarization indices of the virtual photon in the complex-conjugate amplitude and in the amplitude, respectively. The outgoing lepton has the momentum $l^\mu = l^\mu - q^\mu$ and the azimuthal angle ϕ . The incoming parton has the momentum $p^\mu = xP^\mu$. The outgoing hadron h has the azimuthal angle χ and the longitudinal momentum fraction

$$z_f = \frac{P_h \cdot P}{q \cdot P} = z \frac{p_a \cdot P}{q \cdot P}, \quad (2)$$

of the virtual photon momentum. It comes from the fragmentation of a parton $a = q, \bar{q}, g$ in the final state, and $D_1^a(z)$ is the corresponding fragmentation function (FF). Finally, the variable,

$$q_T^2 = \frac{P_{h\perp}^2}{z_f^2} = \frac{\hat{s}\hat{u}}{\hat{t}}, \quad (3)$$

is the characteristic transverse momentum of the process, where the last equality has been expressed in terms the partonic Mandelstam variables,

$$\hat{s} = (p + q)^2, \quad \hat{t} = (p - p_q)^2, \quad \hat{u} = (q - p_q)^2. \quad (4)$$

The leptonic tensor is given by the standard expression,

$$L^{\mu\nu} = 2(l^\mu l^\nu + l^\nu l^\mu) - g^{\mu\nu} Q^2. \quad (5)$$

Following the literature [11], we perform a tensor decomposition,

$$L^{\mu\nu} w_{\mu\nu} = Q^2 \sum_k^{1,2,3,4,8,9} \mathcal{A}_k w_{\mu\nu} \tilde{\mathcal{V}}_k^{\mu\nu}, \quad (6)$$

where

$$\begin{aligned} \tilde{\mathcal{V}}_1^{\mu\nu} &= \frac{1}{2}(2T^\mu T^\nu + X^\mu X^\nu + Y^\mu Y^\nu), \\ \tilde{\mathcal{V}}_2^{\mu\nu} &= T^\mu T^\nu, \\ \tilde{\mathcal{V}}_3^{\mu\nu} &= -\frac{1}{2}(T^\mu X^\nu + X^\mu T^\nu), \\ \tilde{\mathcal{V}}_4^{\mu\nu} &= \frac{1}{2}(T^\mu X^\nu - Y^\mu X^\nu), \\ \tilde{\mathcal{V}}_8^{\mu\nu} &= -\frac{1}{2}(T^\mu Y^\nu + Y^\mu T^\nu), \\ \tilde{\mathcal{V}}_9^{\mu\nu} &= \frac{1}{2}(X^\mu Y^\nu + Y^\mu X^\nu), \end{aligned} \quad (7)$$

are defined in terms of the orthogonal four-vectors normalized as $T^2 = -X^2 = -Y^2 = -Z^2 = 1$. For a later purpose, it is convenient to express them in terms of the partonic Mandelstam variables,¹

$$\begin{aligned} T^\mu &= \frac{1}{Q} \left(q^\mu + \frac{2Q^2}{\hat{s} + Q^2} p^\mu \right), \\ X^\mu &= \sqrt{\frac{\hat{t}}{\hat{s}\hat{u}}} \left[-\frac{\hat{s} + Q^2}{\hat{t}} p_q^\mu - q^\mu - \frac{1}{\hat{s} + Q^2} \left(Q^2 + \frac{\hat{s}\hat{u}}{\hat{t}} \right) p^\mu \right], \\ Z^\mu &= -\frac{q^\mu}{Q}, \\ Y^\mu &= \epsilon^{\mu\nu\rho\sigma} Z_\nu X_\rho T_\sigma. \end{aligned} \quad (8)$$

The coefficients are given by

¹Our conventions for γ_5 and the antisymmetric tensor $\epsilon^{\mu\nu\rho\lambda}$ are the same as in [1,2]: $\gamma_5 = +i\gamma^0\gamma^1\gamma^2\gamma^3$ and $\epsilon_{0123} = 1 = -\epsilon^{0123}$ so that $\text{Tr}[\gamma_5\gamma^0\gamma^1\gamma^2\gamma^3] = -4i$.

$$\begin{aligned}
 A_1 &= 1 + \cosh^2 \psi = \frac{2}{1 - \varepsilon}, \\
 A_2 &= -2, \\
 A_3 &= -\sinh 2\psi \cos \phi_h = -\frac{2\sqrt{2\varepsilon(1+\varepsilon)}}{1 - \varepsilon} \cos \phi_h, \\
 A_4 &= \sinh^2 \psi \cos 2\phi_h = \frac{2\varepsilon}{1 - \varepsilon} \cos 2\phi_h, \\
 A_8 &= -\sinh 2\psi \sin \phi_h = -\frac{2\sqrt{2\varepsilon(1+\varepsilon)}}{1 - \varepsilon} \sin \phi_h, \\
 A_9 &= \sinh^2 \psi \sin 2\phi_h = \frac{2\varepsilon}{1 - \varepsilon} \sin 2\phi_h, \quad (9)
 \end{aligned}$$

where the ‘electron rapidity’ ψ is defined by $\cosh \psi \equiv 2x_B S_{eq}/Q^2 - 1$, and $\phi_h \equiv \phi - \chi$ is the hadron angle relative to the lepton angle (lepton plane). We have introduced in (9) the ratio of the longitudinal/transverse photon fluxes,

$$\varepsilon = \frac{1 - y}{1 - y + \frac{y^2}{2}}, \quad (10)$$

with the standard variable $y = P \cdot q / P \cdot l$ in DIS. Our task is to derive the hard factor $w_{\mu\nu}^a$. The transversely polarized proton can emit either a quark (or an antiquark) or a gluon that initiates hard scattering. We consider the quark-initiated channel in the remainder of this section. The gluon-initiated channel is studied in the next section.

B. Quark-initiated, quark-fragmenting channel

The basic hard scattering processes in the quark-initiated channel include $q\gamma^* \rightarrow qg$ and $\bar{q}\gamma^* \rightarrow \bar{q}g$, where either the (anti)quark or the gluon in the final state fragments into the detected hadron. We first consider the quark fragmenting channel, namely, $a = q$ (or $a = \bar{q}$) in (1). The new approach to SSAs that we pursue was originally developed by Ratcliffe [12] and rediscovered and completed by us [1,2]. It features the following hadronic tensor:

$$\begin{aligned}
 w_{\mu\nu}^q &= \frac{e_q^2}{2} \int dx g_T^q(x) S_{\perp}^{\lambda} \\
 &\times \frac{\partial}{\partial k_{\perp}^{\lambda}} (\delta((k+q-p_q)^2) \text{Tr}[\gamma_5 \not{k} S_{\mu\nu}^{(q)}(k)])_{k=p} + \dots, \quad (11)
 \end{aligned}$$

where $S_{\perp}^{\mu} = (0, \vec{S}_{\perp}, 0) = M_N(0, \cos \Phi_S, \sin \Phi_S, 0)$ is the spin vector of the proton with $S_{\perp}^2 = -M_N^2$. (In [2], we adopted the normalization $S_{\perp}^2 = -1$.) The δ function arises from the on-shell condition for the unobserved gluon with the momentum $k + q - p_q$. The distribution $g_T(x)$ is defined through the matrix element,

$$\int \frac{d\lambda}{4\pi} e^{i\lambda x} \langle PS_{\perp} | \bar{q}(0) \gamma_{\perp}^{\mu} \gamma_5 W q(\lambda n) | PS_{\perp} \rangle = S_{\perp}^{\mu} g_T^q(x), \quad (12)$$

where W denotes the Wilson line connecting $[0, \lambda n]$. Equation (12) already shows that a transverse SSA is proportional to the proton mass $|S_{\perp}| = M_N$, but not the current quark mass m_q as often assumed in perturbative calculations [5]. We set $m_q = 0$ throughout this paper.

In (11), we have employed the Wandzura-Wilczek (WW) approximation and omitted the contribution from the genuine twist-three $q\bar{q}g$ correlation functions. The full expression can be found in [1,2]. While the truncated formula (11) has attractive features such as gauge invariance and infrared finiteness, strictly speaking, the WW approximation is not self-consistent. Our rationale is that, since the hard kernel $S_{\mu\nu}^{(q)}$ is evaluated to $\mathcal{O}(\alpha_s^2)$, the omitted terms in (11) are formally of higher order in α_s , compared to the genuine twist-three contributions previously investigated in the literature [13–17]. The WW part, on the other hand, has no analogue in the usual twist-three approach to SSAs. Moreover, it can be evaluated solely from the knowledge of twist-two PDFs. It thus deserves a focused study.

The imaginary phase necessary for a SSA arises from internal loops in the hard kernel $S_{\mu\nu}^{(q)}(k)$. We assume that it is symmetric in $\mu\nu$, because the leptonic tensor (5) is. Thanks to the factorization property discussed in [1], $S_{\mu\nu}^{(q)}(k)$ is calculable in perturbation theory and infrared finite.² It starts at $\mathcal{O}(\alpha_s^2)$ and involves six topologically different loop diagrams in the $\gamma^* q \rightarrow qg$ amplitude. The tree-level amplitude consists of two diagrams, so there are 12 diagrams at the squared amplitude level (see [2] for the explicit expression). These diagrams have to be computed for a noncolinear incoming parton momentum $k^{\mu} = (xP^+, k_{\perp}, 0)$, and the limit $k_{\perp} \rightarrow 0$ can be taken only after the differentiation with respect to k_{\perp} .³ In [2], we derived (11) by brute force, taking care of the cancellation of infrared divergences from various diagrams. The calculation was quite cumbersome, and the result has not been checked by other means. In this paper, we present a more efficient approach, which can be straightforwardly generalized to the Drell-Yan case.

²The k_{\perp} -derivative in (11) gives

$$\begin{aligned}
 S_{\perp}^{\lambda} \frac{\partial}{\partial k_{\perp}^{\lambda}} \text{Tr}[\gamma_5 \not{k} S_{\mu\nu}^{(q)}(k)] \Big|_{k=p} &= \text{Tr}[\gamma_5 \not{p} S_{\mu\nu}^{(q)}(p)] \\
 &+ S_{\perp}^{\lambda} \text{Tr} \left[\gamma_5 \not{p} \frac{\partial S_{\mu\nu}^{(q)}(k)}{\partial k_{\perp}^{\lambda}} \right]_{k=p}. \quad (13)
 \end{aligned}$$

The first term alone is infrared divergent [18,19]. The divergence is cured by the second term, which takes into account a quark transverse momentum [1,20,21].

³More precisely, we required the on-shell condition $k^2 = 0$ in [1] for the incoming parton in the proof of gauge invariance, which implies $k^- = k_{\perp}^2 / (2k^+) \neq 0$. However, k^- can be neglected for the present purpose, since we only keep terms linear in k_{\perp} .

Our basic observation is that the symmetric tensor,

$$\mathcal{H}_{\mu\nu}(k) \equiv \text{Tr}[\gamma_5 \not{k} S_{\mu\nu}^{(q)}(k)], \quad (14)$$

consists only of the three four-vectors k , q , and p_q and involves the totally antisymmetric tensor because of the presence of γ_5 . Furthermore, it has to satisfy the QED Ward identity $q_\mu \mathcal{H}^{\mu\nu} = 0$. There are only two independent tensor structures that satisfy these criteria,

$$\begin{aligned} T_1^{\mu\nu}(k) &= \left(k^\mu + \frac{k \cdot q}{Q^2} q^\mu \right) \epsilon^{\nu k q p_q} + \left(k^\nu + \frac{k \cdot q}{Q^2} q^\nu \right) \epsilon^{\mu k q p_q}, \\ T_2^{\mu\nu}(k) &= \left(p_q^\mu + \frac{p_q \cdot q}{Q^2} q^\mu \right) \epsilon^{\nu k q p_q} + \left(p_q^\nu + \frac{p_q \cdot q}{Q^2} q^\nu \right) \epsilon^{\mu k q p_q}. \end{aligned} \quad (15)$$

We can thus write

$$\mathcal{H}^{\mu\nu}(k) = T_1^{\mu\nu}(k) S_1(\tilde{s}, \tilde{t}, \tilde{u}, Q^2) + T_2^{\mu\nu}(k) S_2(\tilde{s}, \tilde{t}, \tilde{u}, Q^2). \quad (16)$$

Thanks to the Lorentz covariance, the scalar functions $S_{1,2}$ depend only on Q^2 and the Mandelstam variables,

$$\tilde{s} = (k+q)^2, \quad \tilde{t} = (k-p_q)^2, \quad \tilde{u} = (q-p_q)^2 = \hat{u}, \quad (17)$$

which are the noncollinear generalizations of (4). In terms of these variables, we have

$$\delta((k+q-p_q)^2) = \delta(\tilde{s} + \tilde{t} + \hat{u} - k^2 + Q^2). \quad (18)$$

Since only the terms linear in k_\perp are needed [see (11)], we can ignore any k^2 dependence in the δ function as well as in $\mathcal{H}^{\mu\nu}(k)$.

Given $\mathcal{H}^{\mu\nu}$, we invert the relation (16) to obtain $S_{1,2}$ as

$$\begin{aligned} S_1(\tilde{s}, \tilde{t}, \tilde{u}, Q^2) &= \frac{(\mathcal{H} \cdot T_1)(T_2 \cdot T_2) - (\mathcal{H} \cdot T_2)(T_1 \cdot T_2)}{(T_1 \cdot T_1)(T_2 \cdot T_2) - (T_1 \cdot T_2)^2}, \\ S_2(\tilde{s}, \tilde{t}, \tilde{u}, Q^2) &= \frac{(\mathcal{H} \cdot T_2)(T_1 \cdot T_1) - (\mathcal{H} \cdot T_1)(T_1 \cdot T_2)}{(T_1 \cdot T_1)(T_2 \cdot T_2) - (T_1 \cdot T_2)^2}, \end{aligned} \quad (19)$$

where a shorthand notation $T_1 \cdot T_2 \equiv T_1^{\mu\nu} T_{2\mu\nu}$, etc., have been introduced. The hadronic tensor is then written as

$$\begin{aligned} w_{\mu\nu}^q &= \frac{e_q^2}{2} \int dx \delta(\hat{s} + \hat{t} + \hat{u} + Q^2) \\ &\times \left[x \frac{d g_T^q(x)}{dx} \frac{S_\perp \cdot p_q}{p \cdot (q - p_q)} \mathcal{H}_{\mu\nu}(p) \right. \\ &+ g_T^q(x) \frac{S_\perp \cdot p_q}{p \cdot (q - p_q)} x \frac{\partial \mathcal{H}_{\mu\nu}(p)}{\partial x} \\ &\left. + g_T^q(x) S_\perp^2 \left(\frac{\partial}{\partial k_\perp^2} \mathcal{H}_{\mu\nu}(k) \right)_{k=p} \right], \end{aligned} \quad (20)$$

which follows from (40) in [2] with the partial integration.

We now come to the actual computation of $S_{1,2}$. Because $S_{1,2}$ are functions only of the Mandelstam variables $\tilde{s}, \tilde{t}, \tilde{u}$, it is enough to calculate them for the special case $k = p$, express the result in terms of $\hat{s}, \hat{t}, \hat{u}$, and then make the replacements $\hat{s}, \hat{t}, \hat{u} \rightarrow \tilde{s}, \tilde{t}, \tilde{u}$. This is a tremendous simplification compared to the brute-force calculation in [2], especially because $\mathcal{H}^{\mu\nu}$ involves loop integrals. With this new method, there are only two loop integrals to perform (corresponding to $T_{i=1,2}^{\mu\nu}$) relative to six in [2] (corresponding to the basis tensors $\tilde{\mathcal{V}}_{k=1,2,3,4,8,9}^{\mu\nu}$). Moreover, the integrals themselves are simpler owing to the simpler kinematics $k \rightarrow p$. The details of the calculation is relegated to the Appendix. Here, we show the final expressions,

$$\begin{aligned} \frac{1}{g^4} S_1(\tilde{s}, \tilde{t}, \tilde{u}, Q^2) &= 2C_F \frac{Q^2(\tilde{s} + \tilde{t})}{\tilde{s}\tilde{u}^2} \left[\frac{C_A}{\tilde{s} + Q^2} - C_F \frac{3(Q^2 + \tilde{s}) + \tilde{t}}{(\tilde{s} + Q^2)^2} - (C_A - 2C_F) \frac{1}{\tilde{u}} \ln \left(-\frac{\tilde{t}}{\tilde{s} + Q^2} \right) \right], \\ \frac{1}{g^4} S_2(\tilde{s}, \tilde{t}, \tilde{u}, Q^2) &= 2C_F \frac{Q^2}{\tilde{s}\tilde{u}^2} \left[C_A + C_F \frac{Q^2 + \tilde{s} + 3\tilde{t}}{\tilde{s} + Q^2} + (C_A - 2C_F) \frac{\tilde{t} - \tilde{u}}{\tilde{u}} \ln \left(-\frac{\tilde{t}}{\tilde{s} + Q^2} \right) \right], \end{aligned} \quad (21)$$

where $N_c = 3$ is the number of colors, $C_F = (N_c^2 - 1)/(2N_c)$ and $C_A = N_c$. Importantly, $S_{1,2}$ vanish in the photo-production limit $Q^2 \rightarrow 0$. The vanishing is necessary in order to avoid a kinematic pole in the hard factor $\mathcal{H}^{\mu\nu}$ at $Q^2 = 0$ [see (15) and (16)]. It then immediately follows that, since the terms proportional to q^μ and q^ν in $T_{1,2}^{\mu\nu}$ vanish when contracted with the lepton tensor, asymmetries from the present mechanism (neglecting the genuine twist-three effects) are proportional to Q^2 and hence vanish at $Q^2 = 0$. Unfortunately, part of our previous result in [2] does not pass this consistency check.

Inserting (20) into (1), we find

$$\begin{aligned} \frac{d^6 \Delta \sigma}{dx_B dQ^2 dz_f dq_T^2 d\phi d\chi} &= \frac{\alpha_{em}^2 \alpha_s^2}{16\pi^2 x_B^2 S_{ep}^2 Q^2} \frac{M_N}{q_T} \sum_q e_q^2 \sum_k \mathcal{A}_k \mathcal{S}_k \int \frac{dx}{x} \int \frac{dz}{z} D_1^q(z) \delta\left(\frac{q_T^2}{Q^2} - \left(1 - \frac{1}{\hat{x}}\right) \left(1 - \frac{1}{\hat{z}}\right)\right) \\ &\times \left(x^2 \frac{dg_T^q(x)}{dx} \Delta \hat{\sigma}_{Dk}^{qq} + x g_T^q(x) \Delta \hat{\sigma}_k^{qq}\right), \end{aligned} \quad (22)$$

with the variables

$$\hat{x} \equiv \frac{x_B}{x} = \frac{Q^2}{\hat{s} + Q^2}, \quad \hat{z} \equiv \frac{z_f}{z} = \frac{-\hat{t}}{\hat{s} + Q^2}. \quad (23)$$

Following [2], we have defined the partonic cross sections in (22),

$$\begin{aligned} \frac{g^A M_N}{q_T} \mathcal{S}_k \Delta \hat{\sigma}_{Dk}^{qq} &= \frac{S_\perp \cdot p_q}{p \cdot (q - p_q)} \mathcal{H}_{\mu\nu}(p) \tilde{\mathcal{V}}_k^{\mu\nu}, \\ \frac{g^A M_N}{q_T} \mathcal{S}_k \Delta \hat{\sigma}_k^{qq} &= \left(\frac{S_\perp \cdot p_q}{p \cdot (q - p_q)} x \frac{\partial \mathcal{H}_{\mu\nu}(p)}{\partial x} + \left[S_\perp^\lambda \frac{\partial \mathcal{H}_{\mu\nu}(k)}{\partial k_\perp^\lambda} \right]_{k=p} \right) \tilde{\mathcal{V}}_k^{\mu\nu}, \end{aligned} \quad (24)$$

where $\mathcal{S}_k = \sin(\Phi_S - \chi)$ for $k = 1, 2, 3, 4$, and $\mathcal{S}_k = \cos(\Phi_S - \chi)$ for $k = 8, 9$. This structure arises from the property

$$T_{1,2}^{\mu\nu} \tilde{\mathcal{V}}_{\mu\nu}^k = 0, \quad k = 1, 2, 3, 4, \quad (25)$$

so that we have $\Delta \hat{\sigma}_{Dk=1,2,3,4}^{qq} = 0$, and the explicit derivatives of the $T_{1,2}^{\mu\nu}$ tensors,

$$x \frac{\partial \mathcal{H}^{\mu\nu}(p)}{\partial x} = T_1^{\mu\nu}(p) \left(2S_1(\hat{s}, \hat{t}, \hat{u}, Q^2) + x \frac{\partial}{\partial x} S_1(\hat{s}, \hat{t}, \hat{u}, Q^2) \right) + T_2^{\mu\nu}(p) \left(S_2(\hat{s}, \hat{t}, \hat{u}, Q^2) + x \frac{\partial}{\partial x} S_2(\hat{s}, \hat{t}, \hat{u}, Q^2) \right). \quad (26)$$

The k_\perp derivative is evaluated as

$$\begin{aligned} \left[S_\perp^\lambda \frac{\partial \mathcal{H}^{\mu\nu}(k)}{\partial k_\perp^\lambda} \right]_{k=p} &= \left[S_\perp^\lambda \frac{\partial T_1^{\mu\nu}(k)}{\partial k_\perp^\lambda} \right]_{k=p} S_1(\hat{s}, \hat{t}, \hat{u}, Q^2) + T_1^{\mu\nu}(p) \left[S_\perp^\lambda \frac{\partial}{\partial k_\perp^\lambda} S_1(\tilde{s}, \tilde{t}, \tilde{u}, Q^2) \right]_{k=p} \\ &+ \left[S_\perp^\lambda \frac{\partial T_2^{\mu\nu}(k)}{\partial k_\perp^\lambda} \right]_{k=p} S_2(\hat{s}, \hat{t}, \hat{u}, Q^2) + T_2^{\mu\nu}(p) \left[S_\perp^\lambda \frac{\partial}{\partial k_\perp^\lambda} S_2(\tilde{s}, \tilde{t}, \tilde{u}, Q^2) \right]_{k=p}, \end{aligned} \quad (27)$$

with

$$\begin{aligned} \left[S_\perp^\lambda \frac{\partial T_1^{\mu\nu}(k)}{\partial k_\perp^\lambda} \right]_{k=p} &= S_\perp^\mu \epsilon^{\nu p q p_q} + \left(p^\mu + \frac{p \cdot q}{Q^2} q^\mu \right) \epsilon^{\nu S_\perp q p_q} + (\mu \leftrightarrow \nu), \\ \left[S_\perp^\lambda \frac{\partial T_2^{\mu\nu}(k)}{\partial k_\perp^\lambda} \right]_{k=p} &= \left(p_q^\mu + \frac{P_q \cdot q}{Q^2} q^\mu \right) \epsilon^{\nu S_\perp q p_q} + \left(p_q^\nu + \frac{P_q \cdot q}{Q^2} q^\nu \right) \epsilon^{\mu S_\perp q p_q} = T_2^{\mu\nu}(S_\perp). \end{aligned} \quad (28)$$

For the derivatives on $S_{1,2}$, we exploit the fact that $S_{1,2}$ are functions of the Mandelstam variables as in [22],

$$x \frac{\partial}{\partial x} = (\hat{s} + Q^2) \frac{\partial}{\partial \hat{s}} + \hat{t} \frac{\partial}{\partial \hat{t}}, \quad S_\perp^\lambda \frac{\partial}{\partial k_\perp^\lambda} = -2(S_\perp \cdot p_q) \frac{\partial}{\partial \hat{t}}. \quad (29)$$

Some care is needed to implement these derivatives in practice. According to the definition (17), the k_\perp dependence of the hard factor is solely encoded in \tilde{t} . However, if one uses the δ -function constraint $\tilde{s} + \tilde{t} + \tilde{u} = -Q^2$ to eliminate \tilde{u} or \tilde{t} in

$S_{1,2}(\tilde{s}, \tilde{t}, \tilde{u})$, it may seem that one could artificially modify the k_{\perp} dependence. In the original prescription in [22], all the Mandelstam variables are treated as being independent when the hard factor is differentiated in order to avoid this ambiguity. However, such an approach is not practical in the present case owing to the complexity of the one-loop diagrams. In fact, we have inserted the relation $\tilde{s} + \tilde{t} + \tilde{u} = -Q^2$ in (21) to simplify the calculation. This is nevertheless justified because

$$\left(\frac{S_{\perp} \cdot p_q}{p \cdot (q - p_q)} x \frac{\partial}{\partial x} + S_{\perp}^{\lambda} \frac{\partial}{\partial k_{\perp}^{\lambda}} \right) (\tilde{s} + \tilde{t} + \tilde{u} + Q^2) \Big|_{k=p} = 0, \quad (30)$$

and the hard factor (24) is unaffected by this ambiguity. In other words, one can freely switch between $\tilde{u} \leftrightarrow -\tilde{s} - \tilde{t} - Q^2$ even before taking the derivatives without changing the final result. In practice, this leads to an enormous simplification especially in the Drell-Yan process, where there are more diagrams to calculate.

The hard kernels thus obtained are given by

$$\begin{aligned} \Delta \hat{\sigma}_{D8}^{qq} &= 2C_F(1 - \hat{x}) \left(C_A(1 - \hat{x}) + C_F(\hat{x} - 1 - \hat{z} + 3\hat{x}\hat{z}) + (C_A - 2C_F)(1 - 2\hat{x}) \frac{\hat{z} \ln \hat{z}}{1 - \hat{z}} \right) \frac{Q}{q_T}, \\ \Delta \hat{\sigma}_{D9}^{qq} &= 2C_F(1 - \hat{x})^2 \left(C_A + C_F(1 - 3\hat{z}) - (C_A - 2C_F)(1 - 2\hat{z}) \frac{\ln \hat{z}}{1 - \hat{z}} \right) \frac{Q^2}{q_T^2}, \\ \Delta \hat{\sigma}_1^{qq} &= -3 \frac{1 - \hat{z}}{\hat{z}} \frac{Q}{q_T} \Delta \hat{\sigma}_{D8}^{qq}, \\ \Delta \hat{\sigma}_2^{qq} &= -2 \frac{1 - \hat{z}}{\hat{z}} \frac{Q}{q_T} \Delta \hat{\sigma}_{D8}^{qq}, \\ \Delta \hat{\sigma}_3^{qq} &= -\frac{\hat{x}\hat{z} + (1 - \hat{x})(1 - \hat{z})}{2(1 - \hat{x})\hat{z}} \Delta \hat{\sigma}_{D8}^{qq} - \frac{1 - \hat{z}}{\hat{z}} \frac{Q}{q_T} \Delta \hat{\sigma}_{D9}^{qq}, \\ \Delta \hat{\sigma}_4^{qq} &= \frac{1 - \hat{z}}{\hat{z}} \frac{Q}{q_T} \Delta \hat{\sigma}_{D8}^{qq} - \frac{\hat{x}\hat{z} + (1 - \hat{x})(1 - \hat{z})}{(1 - \hat{x})\hat{z}} \Delta \hat{\sigma}_{D9}^{qq}, \\ \Delta \hat{\sigma}_8^{qq} &= C_F \frac{1}{\hat{z}} \left(C_A(1 - \hat{x})(1 - \hat{x} + \hat{z} - 4\hat{x}\hat{z}) + C_F(-(1 - \hat{x})^2 - \hat{z}(6 - 13\hat{x})(1 - \hat{x}) + \hat{z}^2(3 + \hat{x}(-11 + 6\hat{x}))) \right. \\ &\quad \left. + (C_A - 2C_F)(3 - \hat{z} + \hat{x}(-7 + 4\hat{x} + 2\hat{z})) \frac{\hat{z} \ln \hat{z}}{1 - \hat{z}} \right) \frac{Q}{q_T}, \\ \Delta \hat{\sigma}_9^{qq} &= -2C_F \frac{1 - \hat{x}}{\hat{z}} \left(C_A(1 - \hat{x})(1 - 2\hat{z}) + C_F(-4 + \hat{z}(11 - 5\hat{z}) + \hat{x}(4 - 3\hat{z}(3 - \hat{z}))) \right. \\ &\quad \left. + (C_A - 2C_F)(1 - \hat{z}(3 - \hat{z}) - \hat{x}(1 - 2\hat{z})) \frac{\ln \hat{z}}{1 - \hat{z}} \right) \frac{Q^2}{q_T^2}. \end{aligned} \quad (31)$$

The same expressions hold for the antiquark-initiated channels $\Delta \hat{\sigma}^{\bar{q}} = \Delta \hat{\sigma}^{qq}$. The coefficients $\Delta \hat{\sigma}_{1,\dots,4}$ have been conveniently written as the linear combinations of $\Delta \hat{\sigma}_{D8}^{qq}$ and $\Delta \hat{\sigma}_{D9}^{qq}$. This is thanks to the fact that the relations in (24) for $k = 1, 2, 3, 4$ take a special form,

$$\frac{g^4 M_N}{q_T} S_k \Delta \hat{\sigma}_k^{qq} = \left\{ \left[S_{\perp}^{\lambda} \frac{\partial T_{1,\mu\nu}(k)}{\partial k_{\perp}^{\lambda}} \right]_{k=p} S_1(\hat{s}, \hat{t}, \hat{u}, Q^2) + \left[S_{\perp}^{\lambda} \frac{\partial T_{2,\mu\nu}(k)}{\partial k_{\perp}^{\lambda}} \right]_{k=p} S_2(\hat{s}, \hat{t}, \hat{u}, Q^2) \right\} \tilde{\mathcal{V}}_k^{\mu\nu}, \quad (32)$$

so the hard coefficients $\Delta \hat{\sigma}_k^{qq}$, $k = 1, \dots, 4$ are the linear combinations of $S_{1,2}$ just like $\Delta \hat{\sigma}_{D8,9}^{qq}$ [see Eq. (24)]. We also find $\Delta \hat{\sigma}_2^{qq} = 2\Delta \hat{\sigma}_1^{qq}/3$. It follows by noticing $\tilde{\mathcal{V}}_2^{\mu\nu} = \frac{2}{3}\tilde{\mathcal{V}}_1^{\mu\nu} + Z^{\mu}Z^{\nu} + g^{\mu\nu}$, where the extra terms, $Z^{\mu}Z^{\nu}$ and $g^{\mu\nu}$, decouple owing to the QED Ward identity and to $g_{\mu\nu}T_{1,2}^{\mu\nu}(k) = 0$, respectively.

Compared with our previous result in [2], an exact agreement for $\Delta \hat{\sigma}_2^{qq}$ and $\Delta \hat{\sigma}_{Dk}^{qq}$ ($k = 8, 9$) has been confirmed. However, for $\Delta \hat{\sigma}_{1,3,4,8,9}^{qq}$, only the logarithmic terms agree, and the remainders are different. In particular, $\Delta \hat{\sigma}_1^{qq}$ in [2] does not vanish in the photoproduction limit $Q = 0$, in contradiction with the general observation made below (21).

As a nontrivial check of our revised formulas in (31), it is useful and instructive to make a connection to the *longitudinal* single spin asymmetry recently discussed in [3], which is associated with a longitudinally polarized proton with the spin

vector $S^\mu \approx \delta_+^\mu S^+$. In this case, the hadronic tensor is given by

$$w_{\mu\nu}^q = \frac{1}{2} \frac{S^+}{P^+} e_q^2 \int \frac{dx}{x} \Delta q(x) \delta((p+q-p_q)^2) \text{Tr}[\gamma_5 \not{p} S_{\mu\nu}^{(q)}(p)], \quad (33)$$

where $\Delta q(x)$ is the polarized quark PDF. The hard factor $S_{\mu\nu}^{(q)}$ is in fact exactly the same as for a transverse SSA (11). However, there is no parton transverse momentum k_\perp involved in the longitudinal case; namely, the observable is purely twist two. Inserting (33) into (1) and using (14) and (16), we find that only the $k = 8, 9$ harmonics survive,

$$\begin{aligned} \frac{d^6 \Delta\sigma}{dx_B dQ^2 dz_f dq_T^2 d\phi d\chi} &= \frac{\alpha_{em}^2 \alpha_s^2}{16\pi^2 x_B^2 S_{ep}^2 Q^2} \sum_q e_q^2 \int \frac{dz dx}{z x} D_1^q(z) \Delta q(x) \delta\left(\frac{q_T^2}{Q^2} - \left(1 - \frac{1}{\hat{x}}\right) \left(1 - \frac{1}{\hat{z}}\right)\right) \\ &\times (-\mathcal{A}_8 \Delta\hat{\sigma}_{L8}^{qq} + \mathcal{A}_9 \Delta\hat{\sigma}_{L9}^{qq}), \end{aligned} \quad (34)$$

where

$$\begin{aligned} g^A \Delta\hat{\sigma}_{L8}^{qq} &\equiv -\mathcal{H}_{\mu\nu}(p) \tilde{\mathcal{V}}_8^{\mu\nu}, \\ g^A \Delta\hat{\sigma}_{L9}^{qq} &\equiv \mathcal{H}_{\mu\nu}(p) \tilde{\mathcal{V}}_9^{\mu\nu}. \end{aligned} \quad (35)$$

Switching the variables as $dq_T^2 = dP_{hT}^2/z_f^2$, $dQ^2 = x_B S_{ep} dy$ and integrating over χ , we arrive at

$$\begin{aligned} \frac{d^5 \Delta\sigma}{dx_B dy dz_f dP_{hT}^2 d\phi_h} &= \frac{\pi \alpha_{em}^2}{x_B z_f Q^4} \frac{y}{1-\varepsilon} \sum_q e_q^2 \int \frac{d\hat{x}}{\hat{x}} \Delta q\left(\frac{x_B}{\hat{x}}\right) \frac{d\hat{z}}{\hat{z}} D_1^q\left(\frac{z_f}{\hat{z}}\right) \delta\left(\frac{q_T^2}{Q^2} - \left(1 - \frac{1}{\hat{x}}\right) \left(1 - \frac{1}{\hat{z}}\right)\right) \\ &\times \left(\frac{\alpha_s}{2\pi}\right)^2 \left[\sqrt{2\varepsilon(1+\varepsilon)} \Delta\hat{\sigma}_{L8}^{qq} \sin\phi_h + \varepsilon \Delta\hat{\sigma}_{L9}^{qq} \sin(2\phi_h) \right]. \end{aligned} \quad (36)$$

Comparing the above expression to (2) and (4) in [3], we identify $e_q^2 \Delta\hat{\sigma}_{L8}^{qq} = C_{UL}^{\sin\phi_h, q \rightarrow q}$ and $e_q^2 \Delta\hat{\sigma}_{L9}^{qq} = C_{UL}^{\sin 2\phi_h, q \rightarrow q}$, with C_{UL} 's being given in (18) and (19) in [3]. We find a complete agreement with our result including the sign. Indeed, it follows from (24) and (25) that

$$\Delta\hat{\sigma}_{D8,9}^{qq} = \pm 2(1 - \hat{x}) \Delta\hat{\sigma}_{L8,9}^{qq}, \quad (37)$$

namely, the hard coefficients in the longitudinal SSA and (part of) transverse SSA are proportional to each other as already noticed in [3].

C. Quark-initiated, gluon-fragmenting channel

Next we investigate the gluon fragmentation channel $\gamma^* q \rightarrow qg$ with $g \rightarrow h$. In this case, we write $l_1^\mu \equiv k^\mu + q^\mu - p_q^\mu = P_h^\mu/z$, instead of $p_q^\mu = P_h^\mu/z$. It is convenient to employ the same tensor decomposition for the hard part as in (16), because the hard factors $S_{1,2}$ can then be simply obtained from (21) by the crossing $\tilde{t} \leftrightarrow \tilde{u}$. For the cross section, we apply the replacement $p_q \rightarrow l_1$ everywhere in (22) to get

$$\begin{aligned} \frac{d^6 \Delta\sigma}{dx_B dQ^2 dz_f dq_T^2 d\phi d\chi} &= \frac{\alpha_{em}^2 \alpha_s^2}{16\pi^2 x_B^2 S_{ep}^2 Q^2} \frac{M_N}{q_T} \sum_q e_q^2 \sum_k \mathcal{A}_k \mathcal{S}_k \int \frac{dx}{x} \int \frac{dz}{z} D_1^q(z) \delta\left(\frac{q_T^2}{Q^2} - \left(1 - \frac{1}{\hat{x}}\right) \left(1 - \frac{1}{\hat{z}}\right)\right) \\ &\times \left(x^2 \frac{dg_T^q(x)}{dx} \Delta\hat{\sigma}_{Dk}^{qq} + xg_T^q(x) \Delta\hat{\sigma}_k^{qq} \right), \end{aligned} \quad (38)$$

where the hard coefficients are defined as

$$\begin{aligned}\frac{g^4 M_N}{q_T} S_k \Delta \hat{\sigma}_{Dk}^{gg} &= \frac{S_\perp \cdot l_1}{p \cdot (q - l_1)} \mathcal{H}_{\mu\nu}(p) \tilde{\mathcal{V}}_k^{\mu\nu}, \\ \frac{g^4 M_N}{q_T} S_k \Delta \hat{\sigma}_k^{gg} &= \left(\frac{S_\perp \cdot l_1}{p \cdot (q - l_1)} x \frac{\partial}{\partial x} \mathcal{H}_{\mu\nu}(p) + \left[S_\perp^\lambda \frac{\partial}{\partial k_\perp^\lambda} \mathcal{H}_{\mu\nu}(k) \right]_{k=p} \right) \tilde{\mathcal{V}}_k^{\mu\nu}.\end{aligned}\quad (39)$$

To perform the above contractions, the expressions for $\tilde{\mathcal{V}}_k^{\mu\nu}$ in the partonic variables need to be adjusted accordingly by applying $p_q^\mu \rightarrow l_1^\mu$ to (8). To compute the derivatives, we write $T_{1,2}^{\mu\nu}(k)$ in terms of l_1 by substituting $p_q = k + q - l_1$,

$$\begin{aligned}T_1^{\mu\nu}(k) &= - \left(k^\mu + \frac{k \cdot q}{Q^2} q^\mu \right) \epsilon^{\nu k q l_1} - \left(k^\nu + \frac{k \cdot q}{Q^2} q^\nu \right) \epsilon^{\mu k q l_1}, \\ T_2^{\mu\nu}(k) &= - \left(k^\mu - l_1^\mu + \frac{(k - l_1) \cdot q}{Q^2} q^\mu \right) \epsilon^{\nu k q l_1} - \left(k^\nu - l_1^\nu + \frac{(k - l_1) \cdot q}{Q^2} q^\nu \right) \epsilon^{\mu k q l_1},\end{aligned}\quad (40)$$

which lead to

$$\begin{aligned}x \frac{\partial T_1^{\mu\nu}(p)}{\partial x} &= p^\lambda \frac{\partial T_1^{\mu\nu}(p)}{\partial p^\lambda} = 2T_1^{\mu\nu}(p), \\ x \frac{\partial T_2^{\mu\nu}(p)}{\partial x} &= p^\lambda \frac{\partial T_2^{\mu\nu}(p)}{\partial p^\lambda} = T_1^{\mu\nu}(p) + T_2^{\mu\nu}(p),\end{aligned}\quad (41)$$

and

$$\begin{aligned}\left[S_\perp^\lambda \frac{\partial T_1^{\mu\nu}(k)}{\partial k_\perp^\lambda} \right]_{k=p} &= -S_\perp^\mu \epsilon^{\nu p q l_1} - \left(p^\mu + \frac{p \cdot q}{Q^2} q^\mu \right) \epsilon^{\nu S_\perp q l_1} + (\mu \leftrightarrow \nu), \\ \left[S_\perp^\lambda \frac{\partial T_2^{\mu\nu}(k)}{\partial k_\perp^\lambda} \right]_{k=p} &= -S_\perp^\mu \epsilon^{\nu p q l_1} - \left(p^\mu - l_1^\mu + \frac{(p - l_1) \cdot q}{Q^2} q^\mu \right) \epsilon^{\nu S_\perp q l_1} + (\mu \leftrightarrow \nu).\end{aligned}\quad (42)$$

The explicit expressions for the hard coefficients are found to be

$$\begin{aligned}\Delta \hat{\sigma}_{D8}^{gg} &= -2C_F \frac{(1 - \hat{x})(1 - \hat{z})}{\hat{z}} \left[C_A(1 - \hat{x}) + C_F(-3\hat{x}\hat{z} + 4\hat{x} + \hat{z} - 2) + (C_A - 2C_F)(1 - 2\hat{x}) \frac{(1 - \hat{z}) \ln(1 - \hat{z})}{\hat{z}} \right] \frac{Q}{q_T}, \\ \Delta \hat{\sigma}_{D9}^{gg} &= 2C_F \frac{(1 - \hat{x})^2(1 - \hat{z})^2}{\hat{z}^2} \left(C_A - C_F(2 - 3\hat{z}) + (C_A - 2C_F)(1 - 2\hat{z}) \frac{\ln(1 - \hat{z})}{\hat{z}} \right) \frac{Q^2}{q_T^2}, \\ \Delta \hat{\sigma}_1^{gg} &= -3 \frac{1 - \hat{z}}{\hat{z}} \frac{Q}{q_T} \Delta \hat{\sigma}_{D8}^{gg}, \\ \Delta \hat{\sigma}_2^{gg} &= -2 \frac{1 - \hat{z}}{\hat{z}} \frac{Q}{q_T} \Delta \hat{\sigma}_{D8}^{gg}, \\ \Delta \hat{\sigma}_3^{gg} &= - \frac{\hat{x}\hat{z} + (1 - \hat{x})(1 - \hat{z})}{2(1 - \hat{x})\hat{z}} \Delta \hat{\sigma}_{D8}^{gg} - \frac{1 - \hat{z}}{\hat{z}} \frac{Q}{q_T} \Delta \hat{\sigma}_{D9}^{gg}, \\ \Delta \hat{\sigma}_4^{gg} &= \frac{1 - \hat{z}}{\hat{z}} \frac{Q}{q_T} \Delta \hat{\sigma}_{D8}^{gg} - \frac{\hat{x}\hat{z} + (1 - \hat{x})(1 - \hat{z})}{(1 - \hat{x})\hat{z}} \Delta \hat{\sigma}_{D9}^{gg}, \\ \Delta \hat{\sigma}_8^{gg} &= C_F \frac{1 - \hat{z}}{\hat{z}^2} \left(C_A(1 - \hat{x})(4\hat{x}\hat{z} - 7\hat{x} - \hat{z} + 3) + C_F((\hat{x}(6\hat{x} - 11) + 3)\hat{z}^2 + \hat{x}(7\hat{x} - 6)\hat{z} + 2(11 - 8\hat{x})\hat{x} + \hat{z} - 6) \right. \\ &\quad \left. + (C_A - 2C_F)(\hat{x}(8\hat{x} - 2\hat{z} - 11) + \hat{z} + 3) \frac{(1 - \hat{z}) \ln(1 - \hat{z})}{\hat{z}} \right) \frac{Q}{q_T}, \\ \Delta \hat{\sigma}_9^{gg} &= 2C_F \frac{(1 - \hat{x})(1 - \hat{z})^2}{\hat{z}^3} \left(2C_A(-\hat{x}\hat{z} + \hat{x} + \hat{z} - 1) + C_F(\hat{x}(3\hat{z}(\hat{z} + 2) - 4) - \hat{z}(5\hat{z} + 4) + 4) \right. \\ &\quad \left. + (C_A - 2C_F)(\hat{x}(2 - 4\hat{z}) + \hat{z}(\hat{z} + 3) - 2) \frac{\ln(1 - \hat{z})}{\hat{z}} \right) \frac{Q^2}{q_T^2}.\end{aligned}\quad (43)$$

It is seen that the coefficients $\Delta\hat{\sigma}_2^{gg}$ and $\Delta\hat{\sigma}_{Dk}^{gg}$ with $k = 8, 9$ match exactly (56) in [2]. As to $\Delta\hat{\sigma}_{1,3,4,8,9}^{gg}$, only the logarithmic terms agree, with the remainder being different. We have explicitly cross-checked that starting from our results for $\mathcal{H}_{\mu\nu}$ and calculating the longitudinal SSAs, the resultant hard coefficients [proportional to $\Delta\hat{\sigma}_{D8,9}^{gg}$, cf., (37)] agree exactly with those obtained in [3]. Note that $\Delta\hat{\sigma}_{D8,9}$ in (31) and (43) are related by the crossing symmetry (up to a minus sign for $\Delta\hat{\sigma}_{D8}$) [3],

$$\hat{t} \rightarrow \hat{u}, \quad \hat{z} \rightarrow 1 - \hat{z}, \quad q_T \propto \sqrt{\frac{1 - \hat{z}}{\hat{z}}} \rightarrow \frac{\hat{z}}{1 - \hat{z}} q_T. \quad (44)$$

Interestingly, this symmetry does not hold for $\Delta\hat{\sigma}_{1,2,3,4,8,9}$, since a transverse SSA involves the derivative of a hard factor. More specifically, the derivatives of T_2 for $k = 1, 2, 3, 4$ in (28) and (42) cannot be exactly mapped onto each other by the replacement $p_q \rightarrow p + q - l_1$. As for $k = 8, 9$, $\Delta\hat{\sigma}_{8,9}$ contain the derivatives of $S_{1,2}$.

$$\begin{aligned} w_{\mu\nu}^g &= ie_q^2 \int \frac{dx}{x} \mathcal{G}_{3T}(x) \delta((p + q - p_q)^2) \epsilon^{n\alpha\beta S_\perp} S_{\mu\nu}^{(g)\alpha\beta'}(p) \omega_{\alpha'\alpha} \omega_{\beta'\beta} \\ &\quad - ie_q^2 \int dx \mathcal{G}_{3T}(x) \left(g_\perp^{\beta\lambda} \epsilon^{\alpha P n S_\perp} - g_\perp^{\alpha\lambda} \epsilon^{\beta P n S_\perp} \right) \frac{\partial}{\partial k_\perp^\lambda} \left(\delta((k + q - p_q)^2) S_{\mu\nu\alpha\beta}^{(g)}(k) \right)_{k=p}, \end{aligned} \quad (46)$$

where $g_\perp^{\mu\nu} = g^{\mu\nu} - P^\mu n^\nu - n^\mu P^\nu$ and $\omega^{\mu\nu} = g^{\mu\nu} - P^\mu n^\nu$, and α and β are the polarization indices of the gluon in the complex-conjugate amplitude and in the amplitude, respectively. The explicit expression of the hard factor $S_{\mu\nu\alpha\beta}^{(g)}$ is referred to (58)–(61) of [2]. We rewrite (46) in a way similar to (11). For the first term, we use the identity,

$$\begin{aligned} \epsilon^{n\alpha\beta S_\perp} S_{\mu\nu}^{(g)\alpha\beta'} \omega_{\alpha'\alpha} \omega_{\beta'\beta} &= \epsilon^{n P \beta S_\perp} S_{\mu\nu\beta}^{(g)} - \epsilon^{n P \alpha S_\perp} S_{\mu\nu\alpha}^{(g)} \\ &= -\epsilon^{\alpha\beta S_\perp n} S_{\mu\nu\alpha\beta}^{(g)}, \end{aligned} \quad (47)$$

where the second equality follows from the Schouten identity,

$$(P \cdot n) \epsilon^{\alpha\beta S_\perp n} = n^\alpha \epsilon^{P \beta S_\perp n} + n^\beta \epsilon^{\alpha P S_\perp n}. \quad (48)$$

Applying also the Schouten identity to the second term of (46), we obtain a compact formula,

$$\begin{aligned} w_{\mu\nu}^g &= -ie_q^2 \int \frac{dx}{x} \mathcal{G}_{3T}(x) S_\perp^\lambda \frac{\partial}{\partial k_\perp^\lambda} \\ &\quad \times \left(\delta((k + q - p_q)^2) \epsilon^{\alpha\beta kn} S_{\mu\nu\alpha\beta}^{(g)}(k) \right)_{k=p}. \end{aligned} \quad (49)$$

We then notice that in the present approximation $k^2 \approx 0$, it is permissible to write

III. SSA IN SIDIS, GLUON-INITIATED CHANNEL

In the previous section, we have assumed that the transversely polarized proton emits a quark (or an anti-quark). As it emits a gluon, there is a new contribution to a SSA proportional to the $\mathcal{G}_{3T}(x)$ distribution [23,24],⁴

$$\begin{aligned} &\int \frac{d\lambda}{2\pi} e^{ix\lambda} \langle PS_\perp | F^{n\alpha}(0) W F^{n\beta}(\lambda n) | PS_\perp \rangle \\ &= -\frac{i}{2P^+} x \Delta G(x) \epsilon^{\alpha\beta P n} - ix \mathcal{G}_{3T}(x) \epsilon^{\alpha\beta S_\perp n} + \dots, \end{aligned} \quad (45)$$

which is the gluonic analog of the $g_T(x)$ distribution. The relevant diagrams that provide an imaginary phase have been identified and computed in [2]. In this section, we revisit the calculation following the new approach introduced in the previous section.

A. Gluon-initiated, quark-fragmenting channel

Our starting point is (32) in [2],

$$(k \cdot q) \epsilon^{\alpha\beta kn} S_{\mu\nu\alpha\beta}^{(g)}(k) = (k \cdot n) \epsilon^{\alpha\beta kq} S_{\mu\nu\alpha\beta}^{(g)}(k), \quad (50)$$

where we have employed the Schouten identity and the Ward identity $k^\alpha S_{\mu\nu\alpha\beta}^{(g)} = k^\beta S_{\mu\nu\alpha\beta}^{(g)} = 0$ again. This allows us to write,

$$\begin{aligned} w_{\mu\nu}^g &= e_q^2 \int dx \mathcal{G}_{3T}(x) S_\perp^\lambda \frac{\partial}{\partial k_\perp^\lambda} \\ &\quad \times \left(\delta((k + q - p_q)^2) \frac{-2i}{\tilde{s} + Q^2} \epsilon^{\alpha\beta kq} S_{\mu\nu\alpha\beta}^{(g)}(k) \right)_{k=p}, \end{aligned} \quad (51)$$

for $k \cdot n / k \cdot q = 2x / (\tilde{s} + Q^2)$ commutes with the k_\perp derivative. The form (51) is convenient with the hard part in the brackets consisting only of the vectors k , q , and p_q , so the same argument leading to (16) holds; we employ the trick (50) to eliminate the vector n from the antisymmetric tensor. We then have the parametrization,

⁴Note the absence of the factor 1/2 in our definition of \mathcal{G}_{3T} , because of which the cross section formulas obtained below have different overall coefficients compared to those in other channels. Nevertheless, we stick to the original normalization in our previous works.

$$\begin{aligned}
 \mathcal{H}_{\mu\nu}^{(g)}(k) &\equiv \frac{-2i}{\tilde{s} + Q^2} e^{\alpha\beta kq} S_{\mu\nu\alpha\beta}^{(g)}(k) \\
 &= T_{1\mu\nu}(k) S_1^{(g)}(\tilde{s}, \tilde{t}, \hat{u}, Q^2) + T_{2\mu\nu}(k) S_2^{(g)}(\tilde{s}, \tilde{t}, \hat{u}, Q^2),
 \end{aligned} \tag{52}$$

with the same tensors $T_{1,2}^{\mu\nu}$ as in (15).

Analogous to the quark-initiated case, (51) yields the contribution to the cross section,

$$\begin{aligned}
 \frac{d^6\Delta\sigma}{dx_B dQ^2 dz_f dq_T^2 d\phi d\chi} &= \frac{\alpha_{em}^2 \alpha_s^2}{8\pi^2 x_B^2 S_{ep}^2 Q^2} \frac{M_N}{q_T} \sum_q e_q^2 \sum_k \mathcal{A}_k \mathcal{S}_k \int \frac{dx}{x} \int \frac{dz}{z} D_1^q(z) \delta\left(\frac{q_T^2}{Q^2} - \left(1 - \frac{1}{\hat{x}}\right)\left(1 - \frac{1}{\hat{z}}\right)\right) \\
 &\times \left(x^2 \frac{d\mathcal{G}_{3T}(x)}{dx} \Delta\hat{\sigma}_{Dk}^{gq} + x\mathcal{G}_{3T}(x) \Delta\hat{\sigma}_k^{gq} \right),
 \end{aligned} \tag{53}$$

where the summation is over the quark and antiquark flavors q . The hard coefficients are defined as

$$\begin{aligned}
 \frac{g^4 M_N}{q_T} \mathcal{S}_k \Delta\hat{\sigma}_{Dk}^{gq} &= \frac{S_\perp \cdot p_q}{p \cdot (q - p_q)} \mathcal{H}_{\mu\nu}^{(g)}(p) \tilde{\mathcal{V}}_k^{\mu\nu}, \\
 \frac{g^4 M_N}{q_T} \mathcal{S}_k \Delta\hat{\sigma}_k^{gq} &= \left(\frac{S_\perp \cdot p_q}{p \cdot (q - p_q)} x \frac{\partial \mathcal{H}_{\mu\nu}^{(g)}(p)}{\partial x} + \left[S_\perp^\lambda \frac{\partial \mathcal{H}_{\mu\nu}^{(g)}(k)}{\partial k_\perp^\lambda} \right]_{k=p} \right) \tilde{\mathcal{V}}_k^{\mu\nu}.
 \end{aligned} \tag{54}$$

As in [2], we evaluate $S_{1,2}^{(g)}$ analytically. Again thanks to the new method, the calculation is much simpler. We omit the detailed derivation, since it is similar to the quark case as explained in the Appendix. The result is given by

$$\begin{aligned}
 \frac{1}{g^4} S_1^{(g)}(\tilde{s}, \tilde{t}, \hat{u}, Q^2) &= 2T_R(C_A - 2C_F) \frac{Q^2}{\tilde{t}^3 \hat{u}^3} \left[\frac{\tilde{t} \hat{u}}{(\tilde{s} + Q^2)^2} ((\tilde{t}^2 - \hat{u}^2)(\tilde{s} + \tilde{t}) + 2\tilde{t}^2 \hat{u}) \right. \\
 &\quad \left. + \tilde{t}^2 (\tilde{t} + \tilde{s}) \ln\left(-\frac{\tilde{t}}{Q^2 + \tilde{s}}\right) + \hat{u}^2 (\tilde{t} - \tilde{s}) \ln\left(-\frac{\hat{u}}{Q^2 + \tilde{s}}\right) \right], \\
 \frac{1}{g^4} S_2^{(g)}(\tilde{s}, \tilde{t}, \hat{u}, Q^2) &= 2T_R(C_A - 2C_F) \frac{Q^2 (\tilde{s} + Q^2)}{\tilde{t}^3 \hat{u}^3} \left[\frac{\tilde{t} \hat{u}}{(\tilde{s} + Q^2)^2} (\tilde{t}^2 + \hat{u}^2) \right. \\
 &\quad \left. + \tilde{t}^2 \ln\left(-\frac{\tilde{t}}{Q^2 + \tilde{s}}\right) + \hat{u}^2 \ln\left(-\frac{\hat{u}}{Q^2 + \tilde{s}}\right) \right],
 \end{aligned} \tag{55}$$

from which we arrive at

$$\begin{aligned}
 \Delta\hat{\sigma}_{D8}^{gq} &= 2T_R(C_A - 2C_F) \frac{(1 - \hat{x})^2}{\hat{z}^2} \left[\hat{x} \hat{z} (1 - 2\hat{z}) - (1 - \hat{x}) \ln(1 - \hat{z}) + (1 - \hat{x}) \frac{\hat{z} \ln \hat{z}}{1 - \hat{z}} \right] \frac{Q}{q_T}, \\
 \Delta\hat{\sigma}_{D9}^{gq} &= -2T_R(C_A - 2C_F) \frac{(1 - \hat{x})^3}{\hat{z}^2} \left[2\hat{z} (1 - \hat{z}) - 1 - \frac{(1 - \hat{z}) \ln(1 - \hat{z})}{\hat{z}} - \frac{\hat{z} \ln \hat{z}}{1 - \hat{z}} \right] \frac{Q^2}{q_T^2}, \\
 \Delta\hat{\sigma}_1^{gq} &= -3 \frac{1 - \hat{z}}{\hat{z}} \frac{Q}{q_T} \Delta\hat{\sigma}_{D8}^{gq}, \\
 \Delta\hat{\sigma}_2^{gq} &= -2 \frac{1 - \hat{z}}{\hat{z}} \frac{Q}{q_T} \Delta\hat{\sigma}_{D8}^{gq}, \\
 \Delta\hat{\sigma}_3^{gq} &= -\frac{\hat{x} \hat{z} + (1 - \hat{x})(1 - \hat{z})}{2(1 - \hat{x})\hat{z}} \Delta\hat{\sigma}_{D8}^{gq} - \frac{1 - \hat{z}}{\hat{z}} \frac{Q}{q_T} \Delta\hat{\sigma}_{D9}^{gq}, \\
 \Delta\hat{\sigma}_4^{gq} &= \frac{1 - \hat{z}}{\hat{z}} \frac{Q}{q_T} \Delta\hat{\sigma}_{D8}^{gq} - \frac{\hat{x} \hat{z} + (1 - \hat{x})(1 - \hat{z})}{(1 - \hat{x})\hat{z}} \Delta\hat{\sigma}_{D9}^{gq},
 \end{aligned}$$

$$\begin{aligned}
\Delta\hat{\sigma}_8^{gq} &= T_R(C_A - 2C_F) \frac{1-\hat{x}}{\hat{z}^3} \left[\hat{z}(4 + \hat{x}(-11 + \hat{z} + 2\hat{z}^2 + \hat{x}(7 - 4\hat{z}^2))) \right. \\
&\quad \left. + (1-\hat{x})(3 - 3\hat{z} - \hat{x}(5 - 2\hat{z})) \ln(1-\hat{z}) + (1-\hat{x})(-1 + \hat{x} + 3\hat{z} - 2\hat{x}\hat{z}) \frac{\hat{z} \ln \hat{z}}{1-\hat{z}} \right] \frac{Q}{q_T}, \\
\Delta\hat{\sigma}_9^{gq} &= 2T_R(C_A - 2C_F) \frac{(1-\hat{x})^2}{\hat{z}^3} \left[-2 + 3\hat{z} - (1-\hat{z})(-2\hat{x} + \hat{x}\hat{z} - 2\hat{z}^2(1-\hat{x})) \right. \\
&\quad \left. - (2-\hat{x}(2-\hat{z}) - 2\hat{z}) \frac{(1-\hat{z}) \ln(1-\hat{z})}{\hat{z}} - (1-\hat{x} - \hat{z}(2-\hat{x})) \frac{\hat{z} \ln \hat{z}}{1-\hat{z}} \right] \frac{Q^2}{q_T^2}, \tag{56}
\end{aligned}$$

with $T_R = 1/2$. It is noticed that the hard coefficients $\Delta\hat{\sigma}_{2,9}^{gq}$ and $\Delta\hat{\sigma}_{Dk}^{gq}$, $k = 8, 9$, agree exactly with (66) and (67) in [2] (after the adjustment of the conventional factor of 2). The logarithmic terms of the coefficients $\Delta\hat{\sigma}_{1,3,4,8}^{gq}$ agree with (67) in [2], but the remainder is different.

B. Gluon-initiated, antiquark-fragmenting channel

The hard coefficients in the antiquark fragmenting channel $g \rightarrow \bar{q} \rightarrow h$ are written as [cf. (54)],

$$\begin{aligned}
\frac{g^4 M_N}{q_T} S_k \Delta\hat{\sigma}_{Dk}^{g\bar{q}} &= \frac{S_\perp \cdot l_1}{p \cdot (q - l_1)} \mathcal{H}_{\mu\nu}^{(g)}(p) \tilde{\mathcal{V}}_k^{\mu\nu}, \\
\frac{g^4 M_N}{q_T} S_k \Delta\hat{\sigma}_k^{g\bar{q}} &= \left(\frac{S_\perp \cdot l_1}{p \cdot (q - l_1)} x \frac{\partial}{\partial x} \mathcal{H}_{\mu\nu}^{(g)}(p) + \left[S_\perp^\lambda \frac{\partial}{\partial k_\perp^\lambda} \mathcal{H}_{\mu\nu}^{(g)}(k) \right]_{k=p} \right) \tilde{\mathcal{V}}_k^{\mu\nu}, \tag{57}
\end{aligned}$$

where $l_1^\mu = P_h^\mu/z$ and the crossing $\tilde{t} \leftrightarrow \tilde{u}$ is implied in $\mathcal{H}_{\mu\nu}^{(g)}$. Performing the derivatives as in (41) and (42), we obtain the hard coefficients,

$$\Delta\hat{\sigma}_{Dk}^{g\bar{q}} = \Delta\hat{\sigma}_{Dk}^{gq}, \quad \Delta\hat{\sigma}_k^{g\bar{q}} = \Delta\hat{\sigma}_k^{gq}. \tag{58}$$

The result for $\Delta\hat{\sigma}_{D8,9}^{g\bar{q}}$ can be inferred in a way which manifests the crossing symmetry under (44),

$$\Delta\hat{\sigma}_{D8,9}^{g\bar{q}}(\hat{x}, \hat{z}) = \mp \Delta\hat{\sigma}_{D8,9}^{gq}(\hat{x}, 1-\hat{z}) \Big|_{q_T \rightarrow \hat{z}q_T/(1-\hat{z})}. \tag{59}$$

C. Comparison to the longitudinal polarization case

It is again illustrative to make a comparison to the case with a longitudinally polarized proton, where the hadronic tensor takes the form [cf. (49)],

$$\begin{aligned}
w_{\mu\nu}^g &= -i \frac{e_q^2 S^+}{2 P^+} \int \frac{dx}{x} \Delta G(x) \epsilon^{\alpha\beta P n} S_{\mu\alpha\beta}^{(g)}(p) \\
&= \frac{e_q^2 S^+}{2 P^+} \int \frac{dx}{x} \Delta G(x) \mathcal{H}_{\mu\nu}^{(g)}(p). \tag{60}
\end{aligned}$$

Inserting $\mathcal{H}_{\mu\nu}^{(g)}(p)$ derived above, we find a formula analogous to (36) with the replacement $\Delta q(x) \rightarrow \Delta G(x)$.

It is seen from (54) that the hard coefficients $\Delta\hat{\sigma}_{L8,9}^{gq}$ are related to $\Delta\hat{\sigma}_{D8,9}^{gq}$ via

$$\Delta\hat{\sigma}_{D8,9}^{gq} = \pm 2(1-\hat{x}) \Delta\hat{\sigma}_{L8,9}^{gq}. \tag{61}$$

We observe a perfect agreement $\Delta\hat{\sigma}_{L8}^{gq} = C_{UL}^{\sin\phi_h}$ and $\Delta\hat{\sigma}_{L9}^{gq} = C_{UL}^{\sin(2\phi_h)}$, where C_{UL} 's are given in (18) and (19) (with $g \rightarrow q$) in [3]. In the antiquark fragmentation channel,

$$\Delta\hat{\sigma}_{L8,9}^{g\bar{q}}(\hat{x}, \hat{z}) = \Delta\hat{\sigma}_{L8,9}^{gq}(\hat{x}, \hat{z}) = \mp \Delta\hat{\sigma}_{L8,9}^{gq}(\hat{x}, 1-\hat{z}) \Big|_{q_T \rightarrow \frac{\hat{z}}{1-\hat{z}}q_T}, \tag{62}$$

also confirms the consistency with [3].

IV. SSA IN DRELL-YAN PROCESS

The new mechanism to generate transverse SSAs in SIDIS described in the previous sections has a direct counterpart in the Drell-Yan process, as the two processes are related by crossing symmetry. In this section, we show that the $g_T(x)$ and $\mathcal{G}_{3T}(x)$ distributions generate SSAs in the polarized Drell-Yan process $pp^\uparrow \rightarrow l^+l^-X$ or $\bar{p}p^\uparrow \rightarrow l^+l^-X$. The theoretical framework is entirely similar to that for SIDIS, but there are practical differences owing to the timelike/spacelike nature of a virtual photon.

A. Setup

We first review the basics of the unpolarized Drell-Yan process $pp \rightarrow \gamma^* X \rightarrow l^+ l^- X$ and set up our notations. The important subprocesses include the $q\bar{q}$ annihilation $q(p) + \bar{q}(p') \rightarrow \gamma^*(q)g(p+p'-q)$ and the Compton scattering $q(p) + g(p') \rightarrow \gamma^*(q)q(p+p'-q)$, followed by the subsequent decay of the timelike virtual photon $\gamma^*(q) \rightarrow l^+(l_1)l^-(l_2)$ with $q^2 = Q^2 > 0$. Here, we assign $p^\mu = xP^\mu$, $p'^\mu = x'P'^\mu$, $p^2 = p'^2 = 0$, $l_1^2 = l_2^2 = 0$, and the center-of-mass energy $s = (P + P')^2 \approx 2P \cdot P'$. We assume that the photon transverse momentum is large, $q_\perp \gg \Lambda_{\text{QCD}}$, so that collinear factorization is applicable, but do not assume a particular ordering between q_\perp and Q . The partonic Mandelstam variables are defined as

$$\hat{s} = (p + p')^2 = xx's, \quad \hat{t} = (p - q)^2, \quad \hat{u} = (p' - q)^2. \quad (63)$$

We parametrize the virtual photon momentum in the proton-proton center-of-mass frame as

$$q^\mu = (q^+, \vec{q}_\perp, q^-), \quad q^\pm = \frac{m_\perp}{\sqrt{2}} e^{\pm y}, \quad (64)$$

where $m_\perp = \sqrt{Q^2 + q_\perp^2}$ is the transverse mass, and y is the rapidity. The following relations are useful:

$$\hat{s} + \hat{t} + \hat{u} = Q^2, \quad q_\perp^2 = \frac{\hat{t}\hat{u}}{\hat{s}}, \quad m_\perp^2 = \frac{(\hat{s} + \hat{t})(\hat{s} + \hat{u})}{\hat{s}}. \quad (65)$$

The differential cross section is given by

$$d\sigma = \frac{e^4}{2sQ^4} \frac{d^3 l_1 d^3 l_2}{(2\pi)^3 2l_1^0 (2\pi)^3 2l_2^0} L^{\mu\nu} W_{\mu\nu}, \quad (66)$$

where the hadronic and leptonic tensors take the form,

$$W_{\mu\nu} = \int d^4 y e^{-iq \cdot y} \langle PP' | J_\mu(y) J_\nu(0) | PP' \rangle, \\ L^{\mu\nu} = 4(l_1^\mu l_2^\nu + l_1^\nu l_2^\mu - g^{\mu\nu} l_1 \cdot l_2) = 2(q^\mu q^\nu - l^\mu l^\nu - q^2 g^{\mu\nu}), \quad (67)$$

with $l \equiv l_1 - l_2$. Inserting $1 = \int d^4 q \delta^{(4)}(q - l_1 - l_2)$ and integrating over the phase space of the dilepton, we get

$$\frac{d\sigma}{d^4 q} = \frac{4\pi\alpha_{em}^2}{3sQ^4(2\pi)^4} (q^\mu q^\nu - q^2 g^{\mu\nu}) W_{\mu\nu} = \frac{4\pi\alpha_{em}^2}{3sQ^2(2\pi)^4} W^{\mu\nu} (-g_{\mu\nu}) \\ = \frac{4\pi\alpha_{em}^2}{3sQ^2 N_c} \frac{\alpha_s}{2\pi^2} \int \frac{dx dx'}{x x'} \sum_q e_q^2 (\sigma_{q\bar{q}} q(x) \bar{q}(x') + \sigma_{qg} q(x) G(x') + \sigma_{gq} G(x) q(x')) \delta(\hat{s} + \hat{t} + \hat{u} - Q^2). \quad (68)$$

The second line shows the QCD factorization formula for the unpolarized cross section with the summation over $q = u, d, \bar{u}, \bar{d}, \dots$. The lowest-order cross sections for the $q\bar{q} \rightarrow \gamma^* g$ and $qg \rightarrow \gamma^* q$ subprocesses are

$$\sigma_{q\bar{q}} = 2C_F \left(\frac{\hat{u}}{\hat{t}} + \frac{\hat{t}}{\hat{u}} + \frac{2Q^2 \hat{s}}{\hat{u}\hat{t}} \right), \quad \sigma_{qg} = 2T_R \left(\frac{\hat{s}}{-\hat{t}} + \frac{-\hat{t}}{\hat{s}} - \frac{2Q^2 \hat{u}}{\hat{s}\hat{t}} \right), \quad \sigma_{gq} = 2T_R \left(\frac{\hat{s}}{-\hat{u}} + \frac{-\hat{u}}{\hat{s}} - \frac{2Q^2 \hat{t}}{\hat{s}\hat{u}} \right). \quad (69)$$

As we see in the following subsections, it is necessary to keep the dependence on lepton angles in order to have nonvanishing SSAs from the present mechanism. We thus return to (66) and work in the so-called Collins-Soper (CS) frame [25], in which experimental data are commonly presented. In the CS frame, $q^\mu = (Q, 0, 0, 0)$, and the lepton momenta take the form,

$$l_1^\mu = \frac{Q}{2} (1, \sin\theta_{cs} \cos\phi_{cs}, \sin\theta_{cs} \sin\phi_{cs}, \cos\theta_{cs}), \\ l_2^\mu = \frac{Q}{2} (1, -\sin\theta_{cs} \cos\phi_{cs}, -\sin\theta_{cs} \sin\phi_{cs}, -\cos\theta_{cs}). \quad (70)$$

We thus have

$$\frac{d^3 l_1 d^3 l_2}{l_1^0 l_2^0} = \frac{d^3 q d^3 (\frac{l_1 - l_2}{2})}{(l_1^0)^2} = \frac{1}{2} d^4 q d\Omega, \quad (71)$$

and

$$\frac{d\sigma}{d^4 q d\Omega} = \frac{\alpha_{em}^2}{64\pi^4 s Q^4} L^{\mu\nu} W_{\mu\nu}, \quad (72)$$

with $d\Omega = d\cos\theta_{cs} d\phi_{cs}$. In complete analogy to the SIDIS case (6)–(9), we decompose the lepton tensor (67) in this frame as [26–28]

$$L^{\mu\nu} = 2Q^2 \sum_k \mathcal{A}_k \hat{Y}_k^{\mu\nu}, \quad (73)$$

where

$$\begin{aligned}
 \mathcal{A}_1 &= 1 + \cos^2 \theta_{cs}, & \tilde{\mathcal{V}}_1^{\mu\nu} &= \frac{1}{2}(X^\mu X^\nu + Y^\mu Y^\nu - 2Z^\mu Z^\nu), \\
 \mathcal{A}_2 &= -2, & \tilde{\mathcal{V}}_2^{\mu\nu} &= -Z^\mu Z^\nu, \\
 \mathcal{A}_3 &= \sin 2\theta_{cs} \cos \phi_{cs}, & \tilde{\mathcal{V}}_3^{\mu\nu} &= -\frac{1}{2}(Z^\mu X^\nu + X^\mu Z^\nu), \\
 \mathcal{A}_4 &= \sin^2 \theta_{cs} \cos 2\phi_{cs}, & \tilde{\mathcal{V}}_4^{\mu\nu} &= \frac{1}{2}(-X^\mu X^\nu + Y^\mu Y^\nu), \\
 \mathcal{A}_8 &= -\sin 2\theta_{cs} \sin \phi_{cs}, & \tilde{\mathcal{V}}_8^{\mu\nu} &= \frac{1}{2}(Z^\mu Y^\nu + Y^\mu Z^\nu), \\
 \mathcal{A}_9 &= \sin^2 \theta_{cs} \sin 2\phi_{cs}, & \tilde{\mathcal{V}}_9^{\mu\nu} &= -\frac{1}{2}(X^\mu Y^\nu + Y^\mu X^\nu).
 \end{aligned} \tag{74}$$

and

In the above expressions the orthonormal vectors T, X, Y, Z coincide with $T^\mu = (1, 0, 0, 0)$, $X^\mu = (0, 1, 0, 0)$, $Y^\mu = (0, 0, 1, 0)$ and $Z^\mu = (0, 0, 0, 1)$ in the CS frame. In generic frames, we may write

$$\begin{aligned}
 T^\mu &= \frac{q^\mu}{Q}, \\
 Z^\mu &= \frac{2}{sm_\perp} ((q \cdot P') \tilde{P}^\mu - (q \cdot P) \tilde{P}'^\mu) = \frac{2}{\hat{s}m_\perp} ((q \cdot p') \tilde{p}^\mu - (q \cdot p) \tilde{p}'^\mu), \\
 X^\mu &= -\frac{2Q}{sq_\perp m_\perp} ((q \cdot P') \tilde{P}^\mu + (q \cdot P) \tilde{P}'^\mu) = -\frac{2Q}{\hat{s}q_\perp m_\perp} ((q \cdot p') \tilde{p}^\mu + (q \cdot p) \tilde{p}'^\mu), \\
 Y^\mu &= -\epsilon^{\mu\nu\rho\sigma} X_\nu Z_\rho T_\sigma,
 \end{aligned} \tag{76}$$

with $\tilde{P}^\mu = P^\mu - P \cdot q q^\mu / q^2$, etc.

B. Quark-initiated channel: $q\bar{q}$ annihilation

We now turn to SSAs, assuming that the proton with momentum $P^\mu \approx \delta_\perp^\mu P^+$ is transversely polarized. It emits either a quark or a gluon, which participates in hard scattering. In the collinear kinematics with $q_\perp \gg \Lambda_{\text{QCD}}$, it has been known that SSAs can arise from the genuine twist-three $q\bar{q}g$ and ggg correlation functions [14,16,29,30]. We first demonstrate that the $g_T(x)$ distribution gives rise to a novel source of SSAs, considering the case in which the polarized proton emits a quark. The unpolarized proton emits either an antiquark to proceed with the $q\bar{q}$ annihilation or a gluon to proceed with the Compton scattering. These two cases are studied separately in this and the next subsections.

The derivation of SSAs is completely parallel with that in SIDIS [1]. In the annihilation channel $q\bar{q} \rightarrow \gamma^* g$, by following the same steps as in [1] with trivial modifications, we can immediately derive the hadronic tensor [cf. (11)],

$$\begin{aligned}
 W_{\mu\nu}^{q\bar{q}} &= \sum_q \frac{e_q^2}{4N_c} \int dx g_T^q(x) \int \frac{dx'}{x'} \bar{q}(x') S_\perp^\lambda \\
 &\quad \times \frac{\partial}{\partial k_\perp^\lambda} (\delta((k + p' - q)^2) \text{Tr}[\gamma_5 \not{k} S_{\mu\nu}^{q\bar{q}}(k)])_{k=p} + \dots,
 \end{aligned} \tag{77}$$

where again the genuine twist-three correlators have been neglected. The diagrams contributing to the hard factors $S^{q\bar{q}}$ have been identified in [31] in the context of longitudinal SSAs and are displayed in Fig. 1. For transverse SSAs, the same set of diagrams are relevant, except that we have to compute them for the noncollinear incoming parton momentum $k^\mu = (xP^+, k_\perp, 0)$.

We adopt the same strategy as in SIDIS; the available vectors to construct $S_{\mu\nu}^{q\bar{q}}$ are k, p' and q , and $S_{\mu\nu}^{q\bar{q}}$ has to satisfy the Ward identity $q^\mu S_{\mu\nu}^{q\bar{q}} = 0$. After tracing with a γ_5 , the only allowed tensor structures are

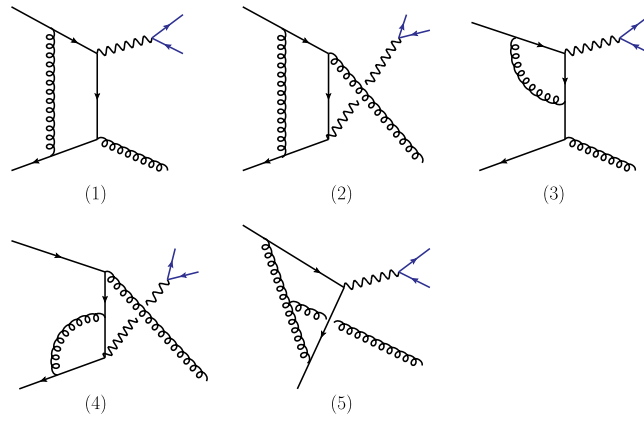


FIG. 1. A class of one-loop diagrams in the $q\bar{q} \rightarrow \gamma^*$ channel that contain imaginary parts. The short blue fermion lines denote the lepton pair from the virtual photon via $\gamma^* \rightarrow l^+l^-$.

$$\begin{aligned}
 \mathcal{H}_{\mu\nu}^{q\bar{q}} &\equiv \text{Tr}[\gamma_5 \not{k} S_{\mu\nu}^{q\bar{q}}(k)] = A^{q\bar{q}}(\tilde{s}, \tilde{t}, \tilde{u}) \left[\left(k_\mu - \frac{q \cdot k}{q^2} q_\mu \right) \epsilon_\nu^{kqp'} + \left(k_\nu - \frac{q \cdot k}{q^2} q_\nu \right) \epsilon_\mu^{kqp'} \right] \\
 &\quad + B^{q\bar{q}}(\tilde{s}, \tilde{t}, \tilde{u}) \left[\left(p'_\mu - \frac{q \cdot p'}{q^2} q_\mu \right) \epsilon_\nu^{kqp'} + \left(p'_\nu - \frac{q \cdot p'}{q^2} q_\nu \right) \epsilon_\mu^{kqp'} \right] \\
 &\equiv A^{q\bar{q}} T_{\mu\nu}^1(k) + B^{q\bar{q}} T_{\mu\nu}^2(k), \tag{78}
 \end{aligned}$$

where $\tilde{s}, \tilde{t}, \tilde{u}$ are the noncollinear ($p \rightarrow k$) versions of the Mandelstam variables in (63). An immediate consequence of (78) is that

$$g^{\mu\nu} W_{\mu\nu}^{q\bar{q}}(k) = 0, \tag{79}$$

namely, the spin-dependent contribution to the cross section (68) integrated over the lepton phase space vanishes. This explains why we need to keep the lepton angles. In contrast, SSAs from the genuine twist-three correlation functions [14,16,29,30] do not vanish after the integration over the lepton angles, which take the form $d\Delta\sigma \sim \vec{S}_\perp \times \vec{q}_\perp$ in the laboratory frame.

Concerning the coefficients $A^{q\bar{q}}$ and $B^{q\bar{q}}$, again it is enough to compute them for the collinear kinematics in (63)

and then implement the replacement $\hat{s}, \hat{t}, \hat{u} \rightarrow \tilde{s}, \tilde{t}, \tilde{u}$. In the case of SIDIS discussed in the previous section, we have calculated the hard factors analytically and demonstrated the efficiency of our new approach. For the Drell-Yan process, in order to save even more efforts and reduce the risk of algebraic errors, we opt to evaluate them using the *Mathematica* package ‘Package-X’ [32]. This allows us to directly obtain the imaginary part of each diagram as a discontinuity in the kinematical variables. The diagrams 1 and 2 in Fig. 1 have cuts in both $\hat{s} > 0$ and $Q^2 > 0$ that need to be added. The diagrams 3, 4, and 5 have cuts only in $Q^2 > 0$. By default, individual diagrams are computed in $4 - 2\epsilon$ dimensions in Package-X and typically contain $1/\epsilon$ poles even in the imaginary parts. These poles must cancel in the end, serving as a consistency check of the result. We find

$$\begin{aligned}
 A^{q\bar{q}}(\tilde{s}, \tilde{t}, \tilde{u}) &= g^4 C_F \left[C_F \frac{2Q^2(3Q^4 - \tilde{s}^2 - 6Q^2\tilde{t} - 2\tilde{s}\tilde{t} + 2\tilde{t}^2)}{(\tilde{s} + \tilde{t})(\tilde{s} + \tilde{u})^2\tilde{t}\tilde{u}} \right. \\
 &\quad \left. - (C_A - 2C_F) \frac{2Q^2}{\tilde{t}^2\tilde{u}^2} \left\{ \frac{Q^2(\tilde{t} - \tilde{u}) - 2\tilde{t}(\tilde{s} + \tilde{t})}{\tilde{s} + \tilde{u}} - \frac{(\tilde{s} + \tilde{t})\tilde{t}}{\tilde{u}} \ln \frac{\tilde{s}}{\tilde{s} + \tilde{u}} - \frac{(\tilde{s} - \tilde{t})\tilde{u}}{\tilde{t}} \ln \frac{\tilde{s}}{\tilde{s} + \tilde{t}} \right\} \right], \tag{80}
 \end{aligned}$$

and $B^{q\bar{q}}(\tilde{s}, \tilde{t}, \tilde{u}) = A^{q\bar{q}}(\tilde{s}, \tilde{u}, \tilde{t})$. Note that $A^{q\bar{q}}$ and $B^{q\bar{q}}$ are proportional to Q^2 , so transverse SSAs vanish in real photon (‘direct’ photon) production with $Q^2 = 0$, similar to the SIDIS case.⁵ The same observation holds for the other channels discussed below. This is not the case for SSAs from the genuine twist-three distributions [14,16,29,30].

⁵Strictly speaking, the CS frame is not defined for $Q = 0$. However, since the hard coefficients are Lorentz invariant, one can still conclude that transverse SSAs vanish in the laboratory frame.

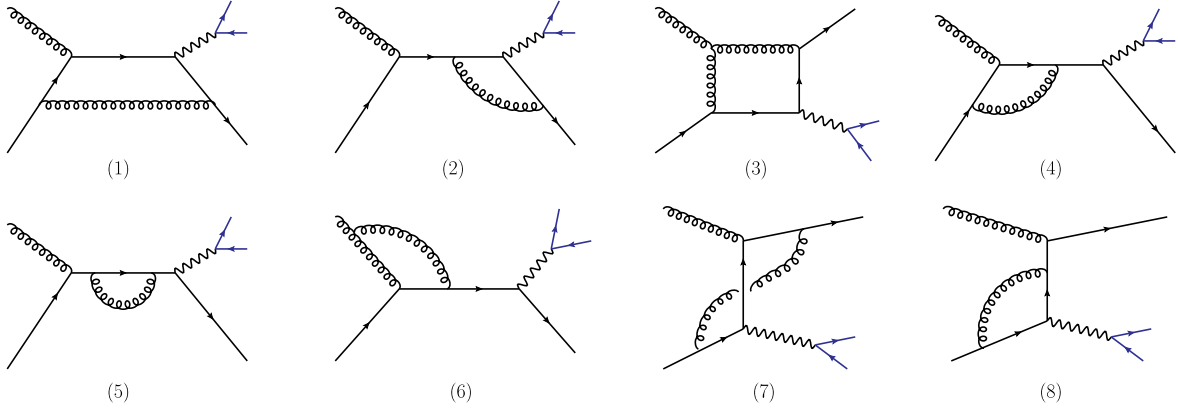


FIG. 2. A class of one-loop diagrams in the $qq \rightarrow q\gamma^*$ channel that contain imaginary parts. The short blue fermion lines denote the lepton pair from the virtual photon via $\gamma^* \rightarrow l^+l^-$.

C. Quark-initiated channel: Compton scattering

Another important subprocess in the Drell-Yan process is the Compton scattering $qq \rightarrow \gamma^*q$, where the gluon comes from the unpolarized proton. The corresponding hadronic tensor takes the form,

$$W_{\mu\nu}^C = \sum_q \frac{e_q^2}{4N_c} \int dx \frac{dx'}{x'} g_T^q(x) G(x') S_{\perp}^{\lambda} \times \frac{\partial}{\partial k_{\perp}^{\lambda}} (\delta(\tilde{s} + \tilde{t} + \tilde{u} - Q^2) \text{Tr}[\gamma_5 \not{k} S_{\mu\nu}^C(k)])_{k=p}, \quad (81)$$

with the unpolarized gluon PDF $G(x)$. As in (78), we adopt the parametrization,

$$\mathcal{H}_{\mu\nu}^C \equiv \text{Tr}[\gamma_5 \not{k} S_{\mu\nu}^C(k)] = A^C(\tilde{s}, \tilde{t}, \tilde{u}) T_{\mu\nu}^1(k) + B^C(\tilde{s}, \tilde{t}, \tilde{u}) T_{\mu\nu}^2(k). \quad (82)$$

In this case, there are eight diagrams that contain imaginary parts as listed in Fig. 2. Diagrams 1, 2, and 3 have discontinuities in both $s > 0$ and $Q^2 > 0$. Diagrams 4, 5, and 6 have discontinuities in $s > 0$, and diagrams 7 and 8 have discontinuities in $Q^2 > 0$. After confirming the cancellation of $1/\epsilon$ poles, we obtain

$$A^C(\tilde{s}, \tilde{t}, \tilde{u}) = g^4 T_R \left[C_F \frac{2Q^2(\tilde{s} + 3\tilde{t} - 4Q^2)}{\tilde{s}\tilde{t}(\tilde{s} + \tilde{u})^2} - (C_A - 2C_F) \frac{2Q^2}{\tilde{s}^3(\tilde{s} + \tilde{u})\tilde{t}^3} \left\{ \tilde{s}\tilde{t}Q^2(\tilde{s} - \tilde{t}) + (\tilde{s} + \tilde{u})(\tilde{s} + \tilde{t}) \left(s^2 \ln \frac{\tilde{s}}{\tilde{s} + \tilde{t}} + \tilde{t}^2 \ln \frac{(\tilde{s} + \tilde{u})(\tilde{s} + \tilde{t})}{\tilde{t}\tilde{u}} \right) \right\} \right],$$

$$B^C(\tilde{s}, \tilde{t}, \tilde{u}) = g^4 T_R \left[-C_F \frac{6Q^2}{\tilde{s}\tilde{t}(\tilde{s} + \tilde{u})} - (C_A - 2C_F) \frac{Q^2}{\tilde{s}^3\tilde{t}^3} \left\{ \frac{\tilde{s}\tilde{t}}{(\tilde{s} + \tilde{t})^2} (Q^2(\tilde{s} + \tilde{t})^2 + 2\tilde{s}\tilde{t}\tilde{u}) + \tilde{s}^2(\tilde{s} + \tilde{u}) \ln \frac{\tilde{s}}{\tilde{s} + \tilde{t}} + \tilde{t}^2(\tilde{s} - \tilde{u}) \ln \frac{(\tilde{s} + \tilde{t})(\tilde{s} + \tilde{u})}{\tilde{t}\tilde{u}} \right\} \right], \quad (83)$$

which vanish for real photon production at $Q = 0$ as mentioned earlier.

D. Crossing symmetry

One might expect that the results for SSAs in SIDIS and in the Drell-Yan process would be related by crossing symmetry. A quick inspection reveals that this is not the case. For example, (21) and (80) are not exactly related by $\tilde{s} \leftrightarrow \tilde{t}$, although some parts are. Even the numbers of

diagrams involved are different in the two cases. The reason is that we are focusing on the imaginary parts of loop diagrams. Because of different kinematics ($q^2 < 0$ or $q^2 > 0$), topologically the same diagrams provide imaginary parts in one case but not in the other. Nevertheless, crossing symmetry should work for the total (real plus imaginary) amplitudes as illustrated in [33], where the authors extracted the imaginary parts of the one-loop amplitudes in SIDIS and the Drell-Yan process from the known one-loop result for $e^+e^- \rightarrow \gamma^* \rightarrow q\bar{q}g$ [34], even

though the latter has no imaginary part. This was achieved by analytically continuing logarithms and dilogarithms, which are the sources of the imaginary parts, into appropriate kinematical regions. As a matter of fact, our direct evaluation of the aforementioned diagrams agrees perfectly with their result inferred by crossing symmetry. Specifically, $A^{q\bar{q}}, B^{q\bar{q}}$ match H_8^a, H_9^a in (4.3) of [33], and A^{qg}, B^{qg} match $H_8^{C_q}, H_9^{C_q}$ in (4.4) of [33] up to overall constants. This might seem surprising at first sight, given that the results in [33] were meant for different observables, i.e., the so-called time-reversal odd (or ‘T-odd’) asymmetries in the *unpolarized* Drell-Yan process via W -boson production, which had been originally analyzed in [35,36]. The equivalence to the present calculation can be understood as follows (see also [3]). The W -boson coupling is proportional to $1 - \gamma_5$. As one picks the ‘1’ term in the amplitude and the γ_5 term in the complex-conjugate amplitude in the unpolarized Drell-Yan process (or DIS), the configuration is equivalent to the

longitudinally polarized Drell-Yan process (or DIS) with photon production (or photon exchange); one can move the γ_5 term from the W -boson vertex to the proton matrix element by repeatedly anticommuting it with γ matrices along a fermion flow. In the case of transverse SSAs, there is an additional complication having to do with the noncollinear kinematics. However, the hard factors $S_{1,2}$ are essentially the same and can be derived via a careful implementation of crossing symmetry [34].

E. Gluon-initiated channel

So far we have assumed that the transversely polarized proton emits a quark. In parallel with our discussion in SIDIS (see Sec. III), the polarized proton can also emit a gluon leading to another contribution to SSAs proportional to the $\mathcal{G}_{3T}(x)$ distribution in the Drell-Yan process. The relevant subprocess is the Compton scattering $qg \rightarrow \gamma^* q$ with the hard factor,

$$\begin{aligned} W_{\mu\nu}^{C(g)} &= -i \sum_q \frac{e_q^2}{2N_c} \int \frac{dx dx'}{x x'} \mathcal{G}_{3T}(x) q(x') S_{\perp}^{\lambda} \frac{\partial}{\partial k_{\perp}^{\lambda}} \left(\delta(\tilde{s} + \tilde{t} + \tilde{u} - Q^2) \epsilon^{\alpha\beta kn} S_{\mu\nu\alpha\beta}^{C(g)}(k) \right)_{k=p} \\ &= \sum_q \frac{e_q^2}{2N_c} \int dx \frac{dx'}{x'} \mathcal{G}_{3T}(x) q(x') S_{\perp}^{\lambda} \frac{\partial}{\partial k_{\perp}^{\lambda}} \left(\delta(\tilde{s} + \tilde{t} + \tilde{u} - Q^2) \frac{-2i}{\tilde{s}} \epsilon^{\alpha\beta kp'} S_{\mu\nu\alpha\beta}^{C(g)}(k) \right)_{k=p}, \end{aligned} \quad (84)$$

which can be compared to (51) and (81). This time we use the relation,

$$k \cdot p' \epsilon^{\alpha\beta kn} S_{\mu\nu\alpha\beta}^{C(g)}(k) = k \cdot n \epsilon^{\alpha\beta kp'} S_{\mu\nu\alpha\beta}^{C(g)}(k), \quad (85)$$

following from the Schouten and Ward identities, to eliminate the vector n . Note that $k \cdot n / k \cdot p' = 2x/\tilde{s}$ commutes with the k_{\perp} derivative.

As before, we parametrize the hard part with two independent tensors,

$$\mathcal{H}_{\mu\nu}^{C(g)} \equiv \epsilon^{\alpha\beta kp'} \frac{-2i}{\tilde{s}} S_{\mu\nu\alpha\beta}^{C(g)}(k) = A^{C(g)} T_{\mu\nu}^1(k) + B^{C(g)} T_{\mu\nu}^2(k). \quad (86)$$

The relevant diagrams are the same as in Fig. 2, but we need to employ the replacement $p \leftrightarrow p'$ (or $\hat{t} \leftrightarrow \hat{u}$) and contract the gluon indices α, β with the antisymmetric tensor $\epsilon^{\alpha\beta pp'}$. The results are

$$\begin{aligned} A^{C(g)}(\tilde{s}, \tilde{t}, \tilde{u}) &= -B^C(\tilde{s}, \tilde{u}, \tilde{t}) - g^A T_R (C_A - 2C_F) \frac{4Q^2(\tilde{s} + \tilde{t})}{\tilde{s}\tilde{u}^3} \left(\frac{(\tilde{s} + 2\tilde{u})\tilde{u}}{(\tilde{s} + \tilde{u})^2} + \ln \frac{\tilde{s}}{\tilde{s} + \tilde{u}} \right), \\ B^{C(g)}(\tilde{s}, \tilde{t}, \tilde{u}) &= -A^C(\tilde{s}, \tilde{u}, \tilde{t}) - g^A T_R (C_A - 2C_F) \frac{4Q^2}{\tilde{s}\tilde{u}^3(\tilde{s} + \tilde{u})} \left(\tilde{s}\tilde{u} + (\tilde{s} + \tilde{u})^2 \ln \frac{\tilde{s}}{\tilde{s} + \tilde{u}} \right). \end{aligned} \quad (87)$$

It is seen that the cross section is for the most part related to the one in the Compton scattering channel (83) via the crossing $\hat{t} \leftrightarrow \hat{u}$, as naively expected. The minus sign is due to $\epsilon^{\mu p q p'} = -\epsilon^{\mu p' q p}$. However, there are extra $\mathcal{O}(1/N_c)$ terms from different contractions of Lorentz indices. Again, the above expressions vanish at $Q = 0$.

F. Summary of the results

After computing the hard factors in all the subprocesses, we can write down the formulas for transverse SSAs. Inserting (73) into (66) and using the formula

$$S_{\perp}^{\lambda} \left(\frac{\partial}{\partial k_{\perp}^{\lambda}} \delta(\tilde{s} + \tilde{t} + \hat{u} - k^2 - Q^2) \right)_{k=p} = - \frac{S_{\perp} \cdot q}{p \cdot (p' - q)} x \frac{\partial}{\partial x} \delta(\hat{s} + \hat{t} + \hat{u} - Q^2), \quad (88)$$

we find

$$\frac{d^6 \sigma^{q\bar{q}}}{d^4 q d\Omega} = \frac{\alpha_{em}^2 \alpha_s^2 M_N}{8\pi^2 N_c s Q^3} \sum_k A_k S_k \sum_q e_q^2 \int \frac{dx}{x} \int \frac{dx'}{x'} \bar{q}(x') \delta(\hat{s} + \hat{t} + \hat{u} - Q^2) \left(x^2 \frac{dg_T(x)}{dx} \Delta \hat{\sigma}_{Dk}^{q\bar{q}} + x g_T^q(x) \Delta \hat{\sigma}_k^{q\bar{q}} \right), \quad (89)$$

$$\frac{d^6 \sigma^C}{d^4 q d\Omega} = \frac{\alpha_{em}^2 \alpha_s^2 M_N}{8\pi^2 N_c s Q^3} \sum_k A_k S_k \sum_q e_q^2 \int \frac{dx}{x} \int \frac{dx'}{x'} G(x') \delta(\hat{s} + \hat{t} + \hat{u} - Q^2) \left(x^2 \frac{dG_T^q(x)}{dx} \Delta \hat{\sigma}_{Dk}^C + x g_T(x) \Delta \hat{\sigma}_k^C \right), \quad (90)$$

$$\frac{d^6 \sigma^{C(g)}}{d^4 q d\Omega} = \frac{\alpha_{em}^2 \alpha_s^2 M_N}{4\pi^2 N_c s Q^3} \sum_k A_k S_k \sum_q e_q^2 \int \frac{dx}{x} \int \frac{dx'}{x'} q(x') \delta(\hat{s} + \hat{t} + \hat{u} - Q^2) \left(x^2 \frac{dG_{3T}(x)}{dx} \Delta \hat{\sigma}_{Dk}^{C(g)} + x G_{3T}(x) \Delta \hat{\sigma}_k^{C(g)} \right), \quad (91)$$

where the partonic cross sections are given by⁶

$$\begin{aligned} \frac{g^4 M_N}{Q} S_k \Delta \hat{\sigma}_{Dk}^i &= \frac{S_{\perp} \cdot q}{p \cdot (p' - q)} \mathcal{H}_{\mu\nu}^i(p) \tilde{\mathcal{V}}_k^{\mu\nu}, \\ \frac{g^4 M_N}{Q} S_k \Delta \hat{\sigma}_k^i &= \left(\frac{S_{\perp} \cdot q}{p \cdot (p' - q)} x \frac{\partial \mathcal{H}_{\mu\nu}^i(p)}{\partial x} + \left[S_{\perp}^{\lambda} \frac{\partial \mathcal{H}_{\mu\nu}^i(k)}{\partial k_{\perp}^{\lambda}} \right]_{k=p} \right) \tilde{\mathcal{V}}_k^{\mu\nu}, \end{aligned} \quad (93)$$

with $i = q\bar{q}, C, C(g)$. We define $S_k = \sin(\Phi_S)$ for $k = 1, 2, 3, 4$ and $S_k = \cos(\Phi_S)$ for $k = 8, 9$.⁷

As in the SIDIS case, we present the partonic cross sections in terms of the new variables,

$$x_a = \frac{Q^2}{2p \cdot q} = \frac{Q^2}{Q^2 - \hat{t}}, \quad x_b = \frac{Q^2}{2p' \cdot q} = \frac{Q^2}{Q^2 - \hat{u}}, \quad c = x_a + x_b - x_a x_b = \frac{Q^2 \hat{s}}{(\hat{s} + \hat{t})(\hat{s} + \hat{u})} = \frac{Q^2}{m_{\perp}^2}, \quad (94)$$

which can be often found in the literature. For the $q\bar{q}$ annihilation channel, we have

$$\begin{aligned} \Delta \hat{\sigma}_{D8}^{q\bar{q}} &= \frac{2C_F \sqrt{c}}{x_a(1-x_b)} \left(2C_F(x_a^2 - x_b^2) + (C_A - 2C_F)x_a x_b \left(-\frac{\ln(c/x_a)}{1-x_a} + \frac{\ln(c/x_b)}{1-x_b} \right) \right), \\ \Delta \hat{\sigma}_{D9}^{q\bar{q}} &= \frac{2C_F}{\sqrt{1-cx_a(1-x_b)}} \left(C_A x_a x_b (2-x_a-x_b) + C_F(x_a(x_a-2)c + x_b(x_b-2)c + x_a^2 + x_b^2) \right. \\ &\quad \left. - (C_A - 2C_F)c \left(x_a(1-x_b) \frac{\ln(c/x_a)}{1-x_a} + (1-x_a)x_b \frac{\ln(c/x_b)}{1-x_b} \right) \right), \end{aligned} \quad (95)$$

⁶Similar to (30), we have the relation

$$\left(\frac{S_{\perp} \cdot q}{p \cdot (p' - q)} x \frac{\partial}{\partial x} + S_{\perp}^{\lambda} \frac{\partial}{\partial k_{\perp}^{\lambda}} \right) (\tilde{s} + \tilde{t} + \tilde{u} - Q^2) \Big|_{k=p} = 0, \quad (92)$$

which allows us to apply the constraint $\tilde{s} + \tilde{t} + \tilde{u} = Q^2$ to the hard factors A^i, B^i before taking the derivatives in (93), as having done already in the previous subsection.

⁷More precisely, $\Phi_S \rightarrow \Phi_S - \phi_{q_{\perp}}$ where $\phi_{q_{\perp}}$ is the azimuthal angle of the virtual photon in the center-of-mass frame. In the CS frame, one sets $\phi_{q_{\perp}} = 0$ as part of the frame definition.

$$\begin{aligned}
\Delta\hat{\sigma}_1^{q\bar{q}} &= \frac{3x_a(1-x_b)}{2x_b\sqrt{1-c}}\Delta\hat{\sigma}_{D8}^{q\bar{q}}, \\
\Delta\hat{\sigma}_2^{q\bar{q}} &= \frac{x_a(1-x_b)}{x_b\sqrt{1-c}}\Delta\hat{\sigma}_{D8}^{q\bar{q}}, \\
\Delta\hat{\sigma}_3^{q\bar{q}} &= -\frac{1}{2}\frac{x_a}{(1-x_a)x_b}\left(\sqrt{c}\Delta\hat{\sigma}_{D8}^{q\bar{q}} + \sqrt{1-c}\Delta\hat{\sigma}_{D9}^{q\bar{q}}\right), \\
\Delta\hat{\sigma}_4^{q\bar{q}} &= \frac{1}{2}\frac{x_a}{(1-x_a)x_b}\left(\sqrt{1-c}\Delta\hat{\sigma}_{D8}^{q\bar{q}} + 2\sqrt{c}\Delta\hat{\sigma}_{D9}^{q\bar{q}}\right), \\
\Delta\hat{\sigma}_8^{q\bar{q}} &= \frac{C_F\sqrt{c}}{x_b(1-c)}\left[-C_Ax_ax_b(c+3x_a(1-x_a)+x_b)+C_F(-c^2(x_b+3)+c(x_a(x_a(5x_a+2)+3)-x_b(3x_b+4)-7)\right. \\
&\quad \left.-9x_a^3+7x_a+7x_b(x_b+1))+(C_A-2C_F)\left(x_a(2x_b+c)\frac{\ln(c/x_a)}{1-x_a}-x_b(2x_a-c)\frac{\ln(c/x_b)}{1-x_b}\right)\right], \\
\Delta\hat{\sigma}_9^{q\bar{q}} &= \frac{C_F}{x_ax_b(1-c)^{3/2}}\left[-C_Ax_ax_b(c^2-cx_a(x_a-3)+c(-3x_b+1)+x_a(1-x_a)-x_b)+C_F(-c^3(x_b+3)\right. \\
&\quad \left.+c^2(x_a(x_a^2-1)+x_b(3x_b+11)+2)-c(2x_a(2x_a(x_a-2)+1)+10x_b^2+x_b-1)-x_a(x_a^2+1)-x_b(x_b+1))\right. \\
&\quad \left.+(C_A-2C_F)c\left(x_a^2(x_a+3)(1-x_b)\frac{\ln(c/x_a)}{1-x_a}+(1-x_a)x_b(2x_a-x_b-c)\frac{\ln(c/x_b)}{1-x_b}\right)\right]. \tag{96}
\end{aligned}$$

For the quark-initiated Compton channel, we get

$$\begin{aligned}
\Delta\hat{\sigma}_{D8}^C &= \frac{2T_Rx_a}{c^{3/2}}\left(-C_Ax_b(c(2-x_b)-x_a-x_b)+C_F(c+x_a)(c-2x_b^2)-(C_A-2C_F)x_a^2x_b(1-x_b)\frac{\ln(1-c)}{c}\right), \\
\Delta\hat{\sigma}_{D9}^C &= \frac{2T_R\sqrt{1-c}x_a}{c(1-x_a)}\left(C_Ax_b(-c+x_a+1)+C_F(c(-x_a+2x_b+1)-2x_a(1-x_a)-4x_b)\right. \\
&\quad \left.+(C_A-2C_F)x_a\left(-\frac{\ln(c/x_a)}{1-x_a}+(1-x_a)x_b\frac{\ln(1-c)}{c}\right)\right), \tag{97}
\end{aligned}$$

$$\begin{aligned}
\Delta\hat{\sigma}_1^C &= \frac{3x_a(1-x_b)}{2x_b\sqrt{1-c}}\Delta\hat{\sigma}_{D8}^C, \\
\Delta\hat{\sigma}_2^C &= \frac{x_a(1-x_b)}{x_b\sqrt{1-c}}\Delta\hat{\sigma}_{D8}^C, \\
\Delta\hat{\sigma}_3^C &= -\frac{1}{2}\frac{x_a}{(1-x_a)x_b}\left(\sqrt{c}\Delta\hat{\sigma}_{D8}^C + \sqrt{1-c}\Delta\hat{\sigma}_{D9}^C\right), \\
\Delta\hat{\sigma}_4^C &= \frac{1}{2}\frac{x_a}{(1-x_a)x_b}\left(\sqrt{1-c}\Delta\hat{\sigma}_{D8}^C + 2\sqrt{c}\Delta\hat{\sigma}_{D9}^C\right), \\
\Delta\hat{\sigma}_8^C &= \frac{T_Rx_a}{(1-x_a)x_b c^{3/2}}\left[-C_Ax_b(c^2(2x_a+2x_b-3)+c(x_a(x_a+6)+x_b+4)-4(x_a^2+x_a+x_b))\right. \\
&\quad \left.+C_F(c^3(4x_a-2)+c^2((x_a-9)x_a+4x_b^2-2x_b-16)+2c(2x_a(x_a+6)+x_b(x_b+12)+8)\right. \\
&\quad \left.-8(x_a(x_a+2)+x_b(x_b+2)))+(C_A-2C_F)x_a^2(1-x_b)\left(c\frac{\ln(c/x_a)}{1-x_a}-x_b(-5c+4x_a)\frac{\ln(1-c)}{c}\right)\right],
\end{aligned}$$

$$\begin{aligned}
\Delta\hat{\sigma}_9^C &= \frac{T_R x_a \sqrt{1-c}}{(1-x_a)^2 x_b c} \left[C_A x_b (2c^2 + c(x_a(2x_a - 5) - 2) + x_a(-3(x_a - 1)x_a - 1)) \right. \\
&\quad + C_F (-2c^2(2x_a^2 - 3x_a + 2x_b + 2) + c(x_a(x_a(5x_a - 18) + 7) + 10x_b - 2) + 2(4x_a^3 + x_a + x_b)) \\
&\quad \left. + (C_A - 2C_F)x_a \left((c(x_a + 4) - x_a) \frac{\ln(c/x_a)}{1-x_a} + (1-x_a)x_b(-5c + 4x_a + x_b) \frac{\ln(1-c)}{c} \right) \right]. \tag{98}
\end{aligned}$$

For the gluon initiated Compton channel, we have

$$\begin{aligned}
\Delta\hat{\sigma}_{D8}^{C(g)} &= \frac{2T_R(1-x_a)x_b}{x_a(1-x_b)c^{3/2}} \left(-C_A(x_a x_b(c(2-x_a) - x_a - x_b) + 2cx_a^2) + C_F(x_b(c+x_b)(c-2x_a^2) + 4cx_a^2) \right. \\
&\quad \left. - (C_A - 2C_F)x_a(1-x_a)x_b^3 \frac{\ln(1-c)}{c} \right), \\
\Delta\hat{\sigma}_{D9}^{C(g)} &= \frac{2T_R(1-x_a)x_b^2 \sqrt{1-c}}{x_a(1-x_b)^2 c} \left(C_A x_a(c-x_b+1) + C_F(c(-2x_a+x_b-1) + 2x_b(1-x_b)) \right. \\
&\quad \left. - (C_A - 2C_F)x_b \left(\frac{\ln(c/x_b)}{1-x_b} + x_a(1-x_b) \frac{\ln(1-c)}{c} \right) \right), \tag{99}
\end{aligned}$$

$$\begin{aligned}
\Delta\hat{\sigma}_1^{C(g)} &= \frac{3x_a(1-x_b)}{2x_b\sqrt{1-c}} \Delta\hat{\sigma}_{D8}^{C(g)}, \\
\Delta\hat{\sigma}_2^{C(g)} &= \frac{x_a(1-x_b)}{x_b\sqrt{1-c}} \Delta\hat{\sigma}_{D8}^{C(g)}, \\
\Delta\hat{\sigma}_3^{C(g)} &= -\frac{1}{2} \frac{x_a}{(1-x_a)x_b} \left(\sqrt{c} \Delta\hat{\sigma}_{D8}^{C(g)} + \sqrt{1-c} \Delta\hat{\sigma}_{D9}^{C(g)} \right), \\
\Delta\hat{\sigma}_4^{C(g)} &= \frac{1}{2} \frac{x_a}{(1-x_a)x_b} \left(\sqrt{1-c} \Delta\hat{\sigma}_{D8}^{C(g)} + 2\sqrt{c} \Delta\hat{\sigma}_{D9}^{C(g)} \right), \\
\Delta\hat{\sigma}_8^{C(g)} &= \frac{T_R}{c^{3/2} x_a(1-x_b)} \left[C_A x_a^2 (-4c^3 + c^2(3-2x_a) + c(x_a - 3x_b^2 - 4x_b - 4) + 4(x_a + x_b) + 4x_b^2) \right. \\
&\quad + C_F (c^3(8x_a^2 + x_b + 6) + c^2(2(x_a - 3)x_a(2x_a + 3) + x_b(3x_b - 10) - 24) \\
&\quad + c(-2x_a^3 + 20x_a^2 + 40x_a + 4x_b(x_b + 8) + 24) - 8(x_a(x_a(x_a + 2) + 3) + x_b(x_b + 3))) \\
&\quad \left. + (C_A - 2C_F)x_a(1-x_a)x_b^2 \left(c \frac{\ln(c/x_b)}{1-x_b} + x_b(c - 4x_b) \frac{\ln(1-c)}{c} \right) \right], \\
\Delta\hat{\sigma}_9^{C(g)} &= \frac{T_R \sqrt{1-c}}{x_a(1-x_b)^2 c} \left[C_A x_a (-4c^3 + c^2(2x_a + 4x_b - 1) + c(x_a - x_b^2 + 5x_b + 3) - 3(x_a + x_b) + x_b^3 - 2x_b^2) \right. \\
&\quad + C_F (8c^3(x_a + 1) + c^2(-2x_a(2x_a + 3) + (x_b - 11)x_b + 6) \\
&\quad + c(-2x_a(x_a + 6) - 3(x_b - 2)(x_b - 1)x_b - 6) + 6x_a(x_a + 1) - 4x_b^3 + 6x_b) \\
&\quad \left. + (C_A - 2C_F)x_b^2 \left((c(x_a - 2) - x_a) \frac{\ln(c/x_b)}{1-x_b} + x_a^2(x_a - 3)(1-x_b) \frac{\ln(1-c)}{c} \right) \right]. \tag{100}
\end{aligned}$$

G. Longitudinal SSA in Drell-Yan Process

Finally, we examine the longitudinal polarization case for a consistency check of the previous results in the literature [7,8,31]. The hard factor in the annihilation channel is written as

$$W_{\mu\nu}^{q\bar{q}} = \sum_q \frac{e_q^2 S^+}{4N_c P^+} \int \frac{dx}{x} \Delta q(x) \int \frac{dx'}{x'} \bar{q}(x') \delta(\hat{s} + \hat{t} + \hat{u} - Q^2) \text{Tr}[\gamma_5 \not{p} S_{\mu\nu}^{q\bar{q}}(p)]. \quad (101)$$

Contracting (78) with the lepton tensor in (73) and noticing $T_{\mu\nu}^{1,2} \tilde{\mathcal{V}}_k^{\mu\nu} = 0$ for $k = 1, 2, 3, 4$, we derive, including the other channels,

$$\begin{aligned} \frac{d\Delta\sigma^{q\bar{q}}}{d^4q d\Omega} &= \frac{\alpha_{em}^2 \alpha_s^2}{8\pi^2 s Q^2 N_c} \sum_q e_q^2 \frac{S^+}{P^+} \int \frac{dx}{x} \Delta q(x) \int \frac{dx'}{x'} \bar{q}(x') \delta(\hat{s} + \hat{t} + \hat{u} - Q^2) \\ &\times (\sin 2\theta_{cs} \sin \phi_{cs} \Delta\hat{\sigma}_{L8}^{q\bar{q}} + \sin^2 \theta_{cs} \sin 2\phi_{cs} \Delta\hat{\sigma}_{L9}^{q\bar{q}}), \end{aligned} \quad (102)$$

$$\begin{aligned} \frac{d\Delta\sigma^C}{d^4q d\Omega} &= \frac{\alpha_{em}^2 \alpha_s^2}{8\pi^2 s Q^2 N_c} \sum_q e_q^2 \frac{S^+}{P^+} \int \frac{dx}{x} \Delta q(x) \int \frac{dx'}{x'} G(x') \delta(\hat{s} + \hat{t} + \hat{u} - Q^2) \\ &\times (\sin 2\theta_{cs} \sin \phi_{cs} \Delta\hat{\sigma}_{L8}^C + \sin^2 \theta_{cs} \sin 2\phi_{cs} \Delta\hat{\sigma}_{L9}^C), \end{aligned} \quad (103)$$

$$\begin{aligned} \frac{d\Delta\sigma^{C(g)}}{d^4q d\Omega} &= \frac{\alpha_{em}^2 \alpha_s^2}{8\pi^2 s Q^2 N_c} \sum_q e_q^2 \frac{S^+}{P^+} \int \frac{dx}{x} \Delta G(x) \int \frac{dx'}{x'} q(x') \delta(\hat{s} + \hat{t} + \hat{u} - Q^2) \\ &\times (\sin 2\theta_{cs} \sin \phi_{cs} \Delta\hat{\sigma}_{L8}^{C(g)} + \sin^2 \theta_{cs} \sin 2\phi_{cs} \Delta\hat{\sigma}_{L9}^{C(g)}), \end{aligned} \quad (104)$$

where

$$\begin{aligned} g^4 \Delta\hat{\sigma}_{L8}^i &= -\tilde{\mathcal{V}}_8^{\mu\nu} (A^i T_{\mu\nu}^1 + B^i T_{\mu\nu}^2) = \frac{\hat{t} \hat{u} (-\hat{s} + \hat{u}) A^i + (\hat{s} + \hat{t}) B^i}{4q_{\perp} m_{\perp}}, \\ g^4 \Delta\hat{\sigma}_{L9}^i &= \tilde{\mathcal{V}}_9^{\mu\nu} (A^i T_{\mu\nu}^1 + B^i T_{\mu\nu}^2) = \frac{\hat{t} \hat{u} ((\hat{s} + \hat{u}) A^i + (\hat{s} + \hat{t}) B^i)}{4Q m_{\perp}}, \end{aligned} \quad (105)$$

with $i = q\bar{q}, C, C(g)$. Comparing (93)–(105), we deduce the relations between the hard coefficients for longitudinal SSAs and the corresponding ones for transverse SSAs,

$$\Delta\hat{\sigma}_{D8,9}^i = \pm 2 \sqrt{\frac{1-c}{c}} \frac{x_b}{1-x_b} \Delta\hat{\sigma}_{L8,9}^i, \quad (106)$$

which verify the agreement with the previous results [7,8].⁸ We collect the explicit formulas below for completeness,

$$\begin{aligned} \Delta\hat{\sigma}_{L8}^{q\bar{q}} &= C_F \frac{-2c}{\sqrt{1-c}} \left[C_F \left(\frac{x_b}{x_a} - \frac{x_a}{x_b} \right) + \frac{C_A - 2C_F}{2} \left(\frac{\ln(c/x_a)}{1-x_a} - \frac{\ln(c/x_b)}{1-x_b} \right) \right], \\ \Delta\hat{\sigma}_{L9}^{q\bar{q}} &= C_F \sqrt{c} \left[C_F \left(\frac{x_a}{x_b} + \frac{x_b}{x_a} \right) - (C_A - 2C_F) \left\{ \frac{1}{1-x_a} \left(1 - \frac{c \ln(c/x_a)}{c-x_a} \right) + \frac{1}{1-x_b} \left(1 - \frac{c \ln(c/x_b)}{c-x_b} \right) \right\} \right], \end{aligned} \quad (107)$$

$$\begin{aligned} \Delta\hat{\sigma}_{L8}^C &= T_R \frac{2(c-x_b)}{\sqrt{1-c}} \left[C_F \left(\frac{x_a}{x_b} - \frac{1+x_a}{2} \right) + \frac{C_A - 2C_F}{2} \left\{ x_b - 1 + \frac{x_a x_b}{c} - \frac{x_a (c-x_b)}{c^2} \ln(1-c) \right\} \right], \\ \Delta\hat{\sigma}_{L9}^C &= T_R \frac{2(c-x_b)}{\sqrt{c}} \left[C_F \left(\frac{x_a}{2x_b} + \frac{1+x_a}{2} \right) + \frac{C_A - 2C_F}{2} \left\{ x_b - \frac{1}{1-x_a} - \frac{x_a \ln(1-c)}{c} + \frac{x_a \ln(c/x_a)}{x_b (1-x_a)^2} \right\} \right], \end{aligned} \quad (108)$$

⁸An earlier work [31] computed the $\mathcal{O}(1/N_c)$ term of $\Delta\hat{\sigma}_{L8}^{q\bar{q}}$ in the annihilation channel. The logarithmic terms agree, but the nonlogarithmic terms do not. This disagreement was already noted in [7].

$$\begin{aligned}\Delta\hat{\sigma}_{L8}^{C(g)} &= \Delta\hat{\sigma}_{L8}^C|_{\hat{t}\leftrightarrow\hat{u}} - T_R(C_A - 2C_F)\frac{2x_a(1-x_a)}{\sqrt{1-c}}, \\ \Delta\hat{\sigma}_{L9}^{C(g)} &= -\Delta\hat{\sigma}_{L9}^C|_{\hat{t}\leftrightarrow\hat{u}} - T_R(C_A - 2C_F)\frac{2x_b(1-x_a)}{\sqrt{c(1-x_b)}}\left(1 - \frac{x_b \ln(c/x_b)}{c-x_b}\right).\end{aligned}\quad (109)$$

A numerical evaluation of the asymmetries was carried out in [8] for the RHIC and J-PARC kinematics with $q_\perp < Q$, which were found to reach up to a few percent in the forward rapidity region.

V. NUMERICAL RESULTS

In this section, we revise our predictions made in [2] for transverse SSAs in SIDIS in light of the corrected formulas presented in Secs. II and III. We then make new predictions for SSAs in the Drell-Yan process based on the results in Sec. IV.

A. Parton distributions

Since we have neglected the genuine twist-three terms initially as indicated by (11) and (77), we should, to be consistent, employ the Wandzura-Wilczek (WW) approximation for the g_T and \mathcal{G}_{3T} distributions,

$$\begin{aligned}xg_T^q(x) &\approx x \int_x^1 dx' \frac{\Delta q(x')}{x'} \quad (\text{WW}), \\ x\mathcal{G}_{3T}(x) &\approx \frac{x}{2} \int_x^1 dx' \frac{\Delta G(x')}{x'} \quad (\text{WW}).\end{aligned}\quad (110)$$

However, there have been recent attempts to constrain the genuine twist-three part of the $g_T(x)$ distribution from a global analysis of the ‘‘worm-gear’’ TMD $g_{1T}(x, k_\perp)$ [9] supplemented with QCD equations of motion [10] and small- x resummation [37]. Motivated by these developments, we try, in addition to (110), two different estimations [10] based on the equation of motion (EOM) and the Lorentz invariant relation (LIR)

$$\begin{aligned}xg_T^q(x) &\approx g_{1T}^{(1)q}(x) \quad (\text{EOM}), \\ xg_T^q(x) &\approx x\Delta q(x) + x \frac{dg_{1T}^{(1)q}(x)}{dx} \quad (\text{LIR}),\end{aligned}\quad (111)$$

where $g_{1T}^{(1)}$ is the second moment of the TMD PDF $g_{1T}(x, k_\perp)$ from [9]. Of course, partly including genuine twist-three corrections this way is not entirely consistent, since we have neglected the other twist-three corrections in (11), (77) from the outset. Still, it is a useful exercise to get a rough estimate of the potential impact of genuine twist-three corrections. According to the derivation of (11) in [1,2], we consider the EOM scenario to be more natural in the present context. However, the LIR scenario cannot be excluded.

We plot $xg_T^{u,d}(x)$ in Fig. 3 and $x^2 dg_T^{u,d}(x)/dx$ in Fig. 4, which enter the computation of SSAs [see, e.g., (89)]. The $g_T^q(x)$ PDFs of the remaining flavors are set to zero in the EOM and LIR scenarios, while they are computed from $\Delta q(x)$ in the WW scenario, for which the result in [38] is adopted. The outcomes in the EOM and LIR scenarios display the importance of the genuine twist-three corrections, although the uncertainty bands are broad. In particular, the PDFs in the LIR scenario are qualitatively different, exhibiting nodes when going from moderate to large x [10], because the (numerical) derivatives of $g_{1T}^{(1)}(x)$ are involved. For $\mathcal{G}_{3T}(x)$, we use $\Delta G(x)$ from [38]. These plots already make clear that SSAs from the $g_T(x)$ distribution can be sizable only when the large- x or valence quark region of the polarized proton is probed (cf., Fig. 6 of [2]).

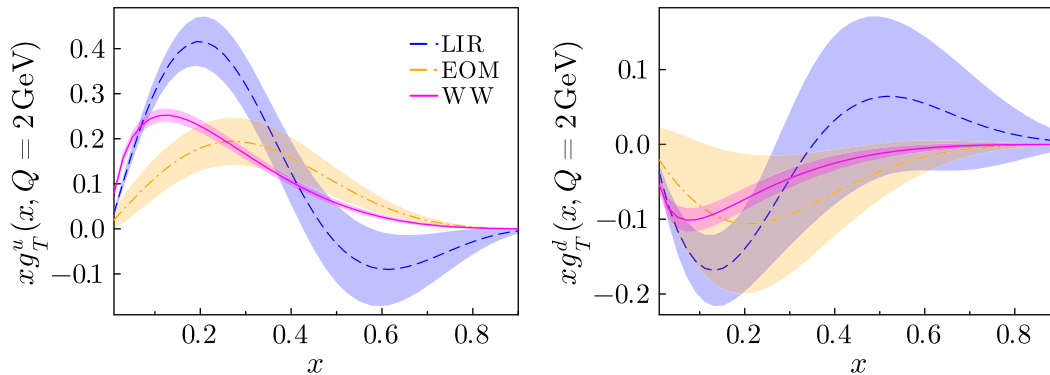


FIG. 3. $xg_T(x)$ for u (left) and d (right) quarks in the three different scenarios defined in (110) and (111). The blue and magenta bands roughly match the blue and magenta bands on Fig. 2 in [10].

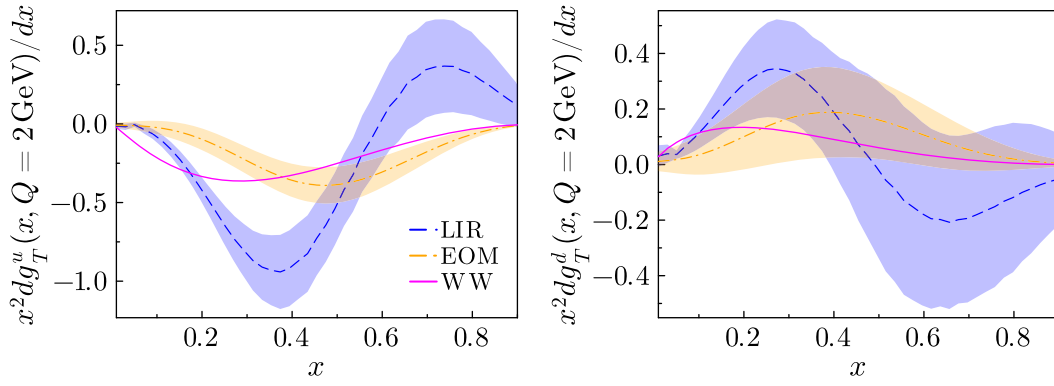


FIG. 4. $x^2 dg_T(x)/dx$ for u and d quarks in the three different scenarios defined in (110) and (111).

For the unpolarized cross section in the denominator, we take the PDFs and FFs in the WW scenario from [39] and [38], respectively, including all the light flavors $q = u, d, s$ and the gluon. In the EOM and LIR scenarios, we take the PDFs from [40] and the FFs from [41] in order to be consistent with [9]. We consider both the proton-proton and pion-proton Drell-Yan reactions. In the latter case, we employ the π^- PDF from [42].

Our numerical evaluations take into account the following sources of uncertainty. The uncertainties in the $g_T^q(x)$ and $\mathcal{G}_{3T}(x)$ PDFs are inherited from $\Delta q(x)$ and $\Delta G(x)$ in the WW scenario and from $g_{1T}^{(1)q}(x)$ in the EOM and LIR scenarios. The $1\text{-}\sigma$ uncertainty from the Monte Carlo replica method is included. Second, we set the factorization and renormalization scales in the PDFs/FFs and the running coupling α_s to ξQ and estimate the scale uncertainty by changing the parameter ξ within $0.5 < \xi < 2$. The described uncertainties are combined in quadrature in the numerical results presented below.

B. SSA in SIDIS revised

We first revise our predictions for SIDIS made in [2]. The calculation is based on the definitions of the SIDIS asymmetries given in (79), (75), (70), and (20) of [2], which are expressed in terms of the $g_T^q(x)$ and $\mathcal{G}_{3T}(x)$ PDFs (and their derivatives) and the hard coefficients having been corrected in Secs. II and III.

We focus on the comparison with Fig. 8 in [2], which was one of the main results there. In Fig. 5, we show the results of all the asymmetries as a function of $P_{h\perp}$ for π^+ (left) and π^- (right), considering the typical EIC kinematics with $\sqrt{S_{ep}} = 45$ GeV, $0.5 < z_f < 0.9$ and $1 < Q^2 < 10$ GeV². We have imposed a lower cut $W > 5$ GeV on $W^2 = (q + P)^2 = Q^2(1 - x_B)/x_B$. The cuts for Fig. 5 are the same as in Fig. 8 of [2] with $P_{hT} \gtrsim 1$ GeV. Comparing the WW result in the left plot of Fig. 5 (for π^+) and the first column in Fig. 8 of [2], we notice that the

Sivers moment $A_{UT}^{\sin(\phi_h - \phi_S)}$ drops to subpercent level, compared to the percent level in Fig. 8 of [2]. The difference is attributed to the correction of the hard coefficient $\Delta\hat{\sigma}_1^i$. Results for the other moments $A_{UT}^{\sin(\phi_h + \phi_S)}$ (Collins asymmetry), $A_{UT}^{\sin(3\phi_h - \phi_S)}$, $A_{UT}^{\sin(\phi_S)}$ and $A_{UT}^{\sin(2\phi_h - \phi_S)}$ are not significantly affected, because they are dominated by the derivative terms (dg_T^q/dx and $d\mathcal{G}_{3T}/dx$), for which the respective hard coefficients $\Delta\hat{\sigma}_{Dk}$ do not change. We observe that the π^- asymmetries are smaller than the π^+ ones in the WW scenario partly owing to $|g_T^u| > |g_T^d|$. Figure 5 also contains new predictions based on $g_T^q(x)$ from the EOM and LIR scenarios, that are not present in [2].

The modifications on the other results in [2] are qualitatively similar and we do not repeat them here. Instead, we explore alternative kinematics to optimize the impact of our new mechanism and find that the asymmetries tend to become larger at lower center-of-mass energies. We show in Fig. 6 new predictions for π^+ as functions of x_B at the EIC with $\sqrt{S_{ep}} = 20$ GeV, $0.01 < y < 0.95$, $0.5 < z_f < 0.9$, and $1 < Q < 10$ GeV, and without a cut on W . Three curves in the left panel correspond to the WW scenario with different lower $P_{h\perp}$ cuts for examining the sensitivity of our predictions to the $P_{hT} \leq 1$ GeV region, where a matching to a TMD computation should be implemented in principle. We find that the asymmetries depend rather sensitively on the choice of the lower P_{hT} cut. The $\sin\phi_S$ and $\sin(2\phi_h - \phi_S)$ asymmetries reach a few percent now and can get even larger after the twist-three corrections are included as shown in the right panel.

C. SSA in Drell-Yan Process

We then present the results for transverse SSAs in the Drell-Yan Process. The spin-dependent part of the cross section can be decomposed as [cf. (74)],

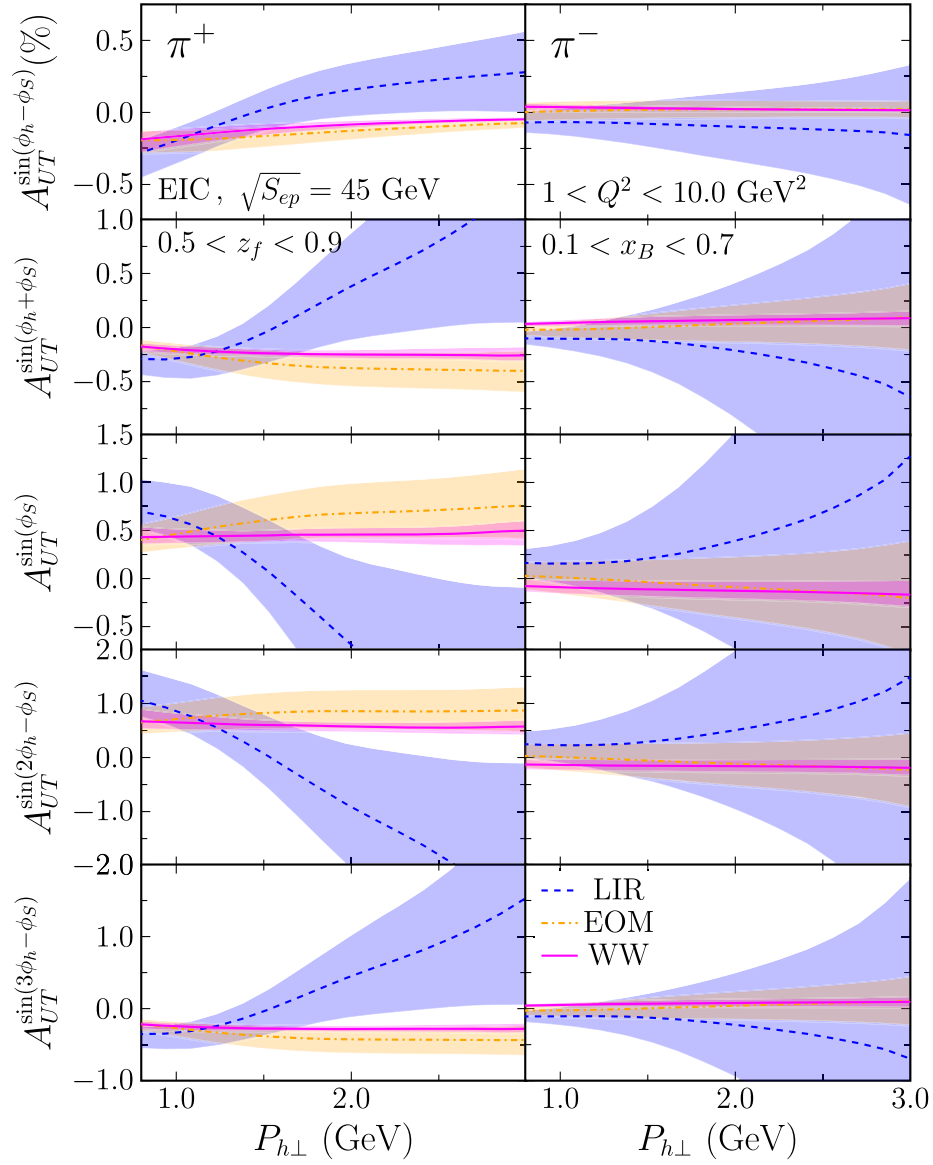


FIG. 5. The $P_{h\perp}$ dependencies of all the SIDIS asymmetries for the EIC kinematics at $\sqrt{S_{ep}} = 45$ GeV in the WW, EOM, and LIR scenarios. Left (right) is for π^+ (π^-).

$$\begin{aligned}
 \frac{d\Delta\sigma}{d^4q d\Omega} &= \sin\Phi_S(\mathcal{F}_1 + \mathcal{F}_2 \cos\phi_{cs} + \mathcal{F}_3 \cos 2\phi_{cs}) + \cos\Phi_S(\mathcal{F}_4 \sin\phi_{cs} + \mathcal{F}_5 \sin 2\phi_{cs}) \\
 &= F^{\sin\Phi_S} \sin\Phi_S + F^{\sin(\phi+\Phi_S)} \sin(\phi_{cs} + \Phi_S) + F^{\sin(\phi_{cs}-\Phi_S)} \sin(\phi_{cs} - \Phi_S) \\
 &\quad + F^{\sin(2\phi_{cs}+\Phi_S)} \sin(2\phi_{cs} + \Phi_S) + F^{\sin(2\phi_{cs}-\Phi_S)} \sin(2\phi_{cs} - \Phi_S),
 \end{aligned} \tag{112}$$

where

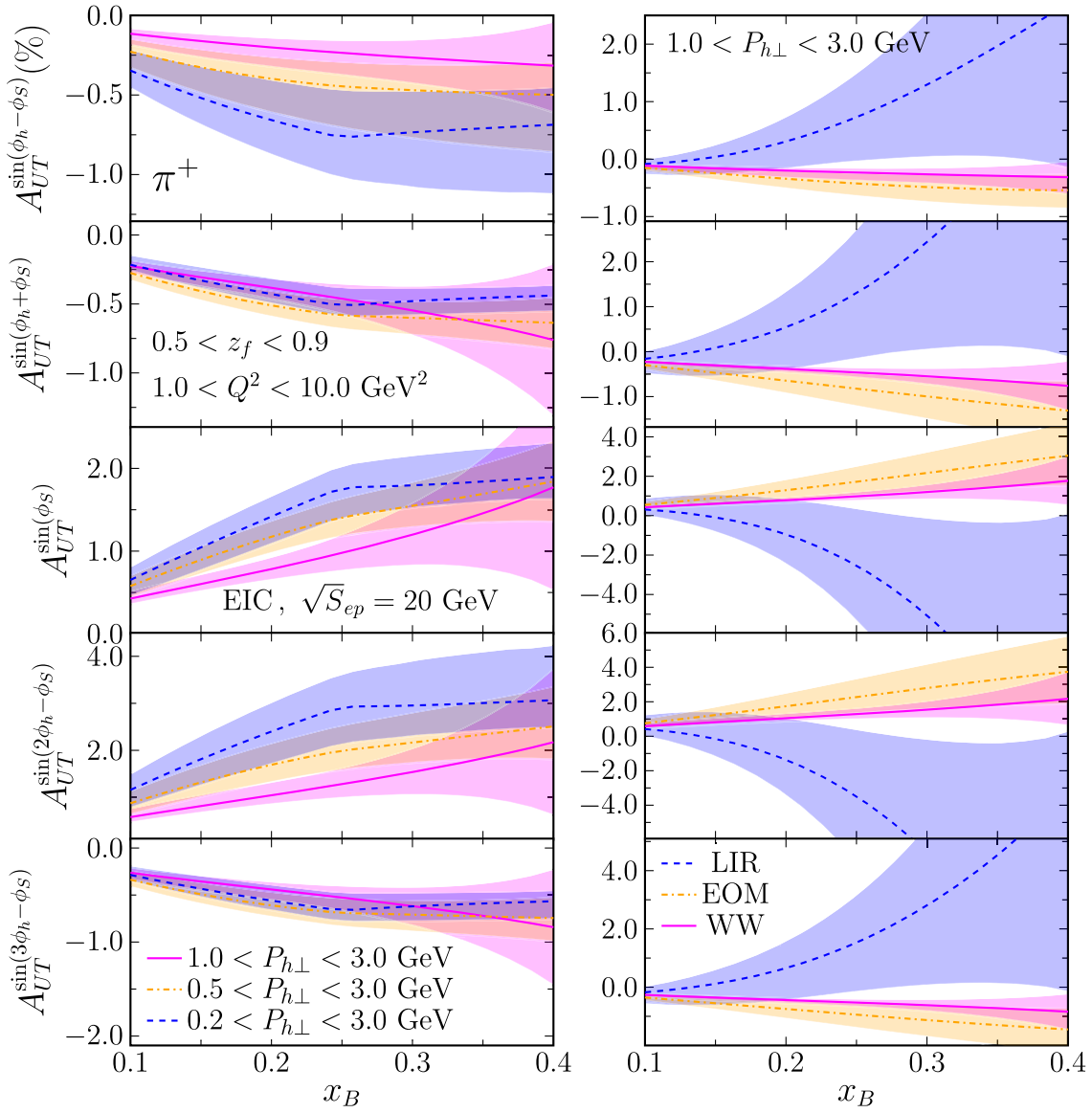


FIG. 6. The x_B dependencies of all the SIDIS π^+ asymmetries for the EIC kinematics at $\sqrt{S_{ep}} = 20$ GeV. Left: different lower $P_{h\perp}$ cutoffs in the WW scenario. Right: different scenarios.

$$\begin{aligned}
 F^{\sin \Phi_S} &= \mathcal{F}_1, \\
 F^{\sin(\phi_{cs} + \Phi_S)} &= \frac{1}{2}(\mathcal{F}_2 + \mathcal{F}_4), \\
 F^{\sin(\phi_{cs} - \Phi_S)} &= \frac{1}{2}(-\mathcal{F}_2 + \mathcal{F}_4), \\
 F^{\sin(2\phi_{cs} + \Phi_S)} &= \frac{1}{2}(\mathcal{F}_3 + \mathcal{F}_5), \\
 F^{\sin(2\phi_{cs} - \Phi_S)} &= \frac{1}{2}(-\mathcal{F}_3 + \mathcal{F}_5).
 \end{aligned} \tag{113}$$

Explicitly, we write

$$\begin{aligned}
\mathcal{F}_1 &= \frac{3}{8} \alpha_s \mathcal{F}_0 \int \frac{dx}{x} \int \frac{dx'}{x'} \delta(\hat{s} + \hat{t} + \hat{u} - Q^2) \sum_q e_q^2 \\
&\quad \times \left(1 + \cos^2 \theta_{cs} - \frac{4}{3} \right) \left[\bar{q}(x') x g_T^q(x) \Delta \hat{\sigma}_1^{q\bar{q}} + G(x') x g_T^q(x) \Delta \hat{\sigma}_1^C + 2q(x') x \mathcal{G}_{3T}(x) \Delta \hat{\sigma}_1^{C(g)} \right] \\
\mathcal{F}_2 &= \frac{3}{8} \alpha_s \mathcal{F}_0 \int \frac{dx}{x} \int \frac{dx'}{x'} \delta(\hat{s} + \hat{t} + \hat{u} - Q^2) \sum_q e_q^2 \\
&\quad \times \sin 2\theta_{cs} \left[\bar{q}(x') x g_T^q(x) \Delta \hat{\sigma}_3^{q\bar{q}} + G(x') x g_T^q(x) \Delta \hat{\sigma}_3^C + 2q(x') x \mathcal{G}_{3T}(x) \Delta \hat{\sigma}_3^{C(g)} \right], \\
\mathcal{F}_3 &= \frac{3}{8} \alpha_s \mathcal{F}_0 \int \frac{dx}{x} \int \frac{dx'}{x'} \delta(\hat{s} + \hat{t} + \hat{u} - Q^2) \sum_q e_q^2 \\
&\quad \times \sin^2 \theta_{cs} \left[\bar{q}(x') x g_T^q(x) \Delta \hat{\sigma}_4^{q\bar{q}} + G(x') x g_T^q(x) \Delta \hat{\sigma}_4^C + 2q(x') x \mathcal{G}_{3T}(x) \Delta \hat{\sigma}_4^{C(g)} \right], \\
\mathcal{F}_4 &= \frac{3}{8} \alpha_s \mathcal{F}_0 \int \frac{dx}{x} \int \frac{dx'}{x'} \delta(\hat{s} + \hat{t} + \hat{u} - Q^2) \sum_q e_q^2 \\
&\quad \times (-\sin 2\theta_{cs}) \left[\bar{q}(x') \left(x^2 \frac{dg_T^q}{dx} \Delta \hat{\sigma}_{D8}^{q\bar{q}} + x g_T^q(x) \Delta \hat{\sigma}_8^{q\bar{q}} \right) + G(x') \left(x^2 \frac{dg_T^q}{dx} \Delta \hat{\sigma}_{D8}^C + x g_T^q(x) \Delta \hat{\sigma}_8^C \right) \right. \\
&\quad \left. + 2q(x') \left(x^2 \frac{d\mathcal{G}_{3T}}{dx} \Delta \hat{\sigma}_{D8}^{C(g)} + x \mathcal{G}_{3T}(x) \Delta \hat{\sigma}_8^{C(g)} \right) \right], \\
\mathcal{F}_5 &= \frac{3}{8} \alpha_s \mathcal{F}_0 \int \frac{dx}{x} \int \frac{dx'}{x'} \delta(\hat{s} + \hat{t} + \hat{u} - Q^2) \sum_q e_q^2 \\
&\quad \times \sin^2 \theta_{cs} \left[\bar{q}(x') \left(x^2 \frac{dg_T^q}{dx} \Delta \hat{\sigma}_{D9}^{q\bar{q}} + x g_T^q(x) \Delta \hat{\sigma}_9^{q\bar{q}} \right) + G(x') \left(x^2 \frac{dg_T^q}{dx} \Delta \hat{\sigma}_{D9}^C + x g_T^q(x) \Delta \hat{\sigma}_9^C \right) \right. \\
&\quad \left. + 2q(x') \left(x^2 \frac{d\mathcal{G}_{3T}}{dx} \Delta \hat{\sigma}_{D9}^{C(g)} + x \mathcal{G}_{3T}(x) \Delta \hat{\sigma}_9^{C(g)} \right) \right], \tag{114}
\end{aligned}$$

with

$$\mathcal{F}_0 = \frac{\alpha_{em}^2 \alpha_s M_N}{3s Q^3 \pi^2 N_c}. \tag{115}$$

In \mathcal{F}_1 , we have eliminated $\Delta \hat{\sigma}_2^i$, $i = q\bar{q}, C, C(g)$, by means of the relation $\Delta \hat{\sigma}_2^i = 2\Delta \hat{\sigma}_1^i/3$. As a consequence, the θ_{cs} dependence has been altered from the more familiar form $1 + \cos^2 \theta_{cs}$. Note that $\int_{-1}^1 d \cos \theta_{cs} (\cos^2 \theta_{cs} - 1/3) = 0$, namely, the asymmetries will vanish if the lepton angles θ_{cs}, ϕ_{cs} are integrated over as already mentioned.

The COMPASS Collaboration has reported in [43,44] the first measurements of transverse SSAs in the pion-induced Drell-Yan Process. In their work, the asymmetries in the CS frame are normalized by the unpolarized cross section which, in the COMPASS kinematics $Q \gg q_\perp$, exhibits the angular distribution,

$$\frac{1}{\sigma} \frac{d\sigma}{d\Omega} = \frac{3}{16\pi} \left(\frac{Q^2 + \frac{3}{2} q_\perp^2}{Q^2 + q_\perp^2} + \frac{Q^2 - \frac{1}{2} q_\perp^2}{Q^2 + q_\perp^2} \cos^2 \theta_{cs} + \dots \right) \approx \frac{3}{16\pi} (1 + \cos^2 \theta_{cs}). \tag{116}$$

Following the expectation based on TMDs [27], they assumed $\mathcal{F}_1 \propto 1 + \cos^2 \theta_{cs}$, so that the θ_{cs} dependence drops out in the $\sin \Phi_S$ asymmetry, whereas the $\sin(2\phi_{cs} \pm \Phi_S)$ harmonics come with the prefactor $\sin^2 \theta_{cs}/(1 + \cos^2 \theta_{cs}^2)$. The $\sin(\phi_{cs} \pm \Phi_S)$ harmonics have been neglected, since they do not arise from twist-two TMDs [27]. In this paper we do not assume that q_\perp is small compared to Q . Besides, in the present mechanism, \mathcal{F}_1 is not proportional to $1 + \cos^2 \theta_{cs}$ as we have seen. It is then more convenient to normalize the asymmetries using the angular-integrated cross section (68). We thus define

$$\begin{aligned} \frac{3}{16\pi} d^{\alpha,\beta}(\theta_{cs}) A_{UT}^{\sin(\alpha\phi_{cs} + \beta\Phi_S)}(Q, q_{\perp}, y) &\equiv \frac{2 \int_0^{2\pi} d\phi_{cs} \int_0^{2\pi} \frac{d\Phi_S}{2\pi} \sin(\alpha\phi_{cs} + \beta\Phi_S) [d\sigma(\phi_{cs}, \Phi_S) - d\sigma(\phi_{cs}, \Phi_S + \pi)]}{\frac{1}{2} \int_{-1}^1 d \cos \theta_{cs} \int_0^{2\pi} d\phi_{cs} \int_0^{2\pi} \frac{d\Phi_S}{2\pi} [d\sigma(\phi_{cs}, \Phi_S) + d\sigma(\phi_{cs}, \Phi_S + \pi)]} \\ &= \left(\frac{d\sigma}{d^4 q} \right)^{-1} 2 \int_0^{2\pi} d\phi_{cs} \int_0^{2\pi} \frac{d\Phi_S}{2\pi} \sin(\alpha\phi_{cs} + \beta\Phi_S) d\sigma(\phi_{cs}, \Phi_S), \end{aligned} \quad (117)$$

where $d\sigma(\phi_{cs}, \Phi_S) \equiv \frac{d\sigma}{d^4 q d\Omega}$. The ‘depolarization factors’ are defined as $d^{0,1}(\theta_{cs}) = \cos^2 \theta_{cs} - 1/3$, $d^{1,\pm 1}(\theta_{cs}) = \sin 2\theta_{cs}$, and $d^{2,\pm 1}(\theta_{cs}) = \sin^2 \theta_{cs}$. The above relations yield

$$A_{UT}^{\sin \Phi_S} = \frac{\alpha_s M_N}{Q} \frac{\sum_q e_q^2 \left[\bar{q}(x') x g_T^q(x) \Delta \hat{\sigma}_1^{q\bar{q}} + G(x') x g_T^q(x) \Delta \hat{\sigma}_1^C + 2q(x') x \mathcal{G}_{3T}(x) \Delta \hat{\sigma}_1^{C(g)} \right]}{\sum_q e_q^2 (\sigma_{q\bar{q}} q(x) \bar{q}(x') + \sigma_{qg} q(x) G(x') + \sigma_{gq} G(x) q(x'))}, \quad (118)$$

$$A_{UT}^{\sin(\phi_{cs} \pm \Phi_S)} = \frac{\alpha_s M_N}{Q} \frac{\frac{1}{2} \sum_q e_q^2 \left[\pm \bar{q}(x') x g_T^q(x) \Delta \hat{\sigma}_3^{q\bar{q}} - \bar{q}(x') (x^2 \frac{dg_T^q}{dx} \Delta \hat{\sigma}_{D8}^{q\bar{q}} + x g_T^q(x) \Delta \hat{\sigma}_8^{q\bar{q}}) + \dots \right]}{\sum_q e_q^2 (\sigma_{q\bar{q}} q(x) \bar{q}(x') + \sigma_{qg} q(x) G(x') + \sigma_{gq} G(x) q(x'))}, \quad (119)$$

$$A_{UT}^{\sin(2\phi_{cs} \pm \Phi_S)} = \frac{\alpha_s M_N}{Q} \frac{\frac{1}{2} \sum_q e_q^2 \left[\pm \bar{q}(x') x g_T^q(x) \Delta \hat{\sigma}_4^{q\bar{q}} + \bar{q}(x') (x^2 \frac{dg_T^q}{dx} \Delta \hat{\sigma}_{D9}^{q\bar{q}} + x g_T^q(x) \Delta \hat{\sigma}_9^{q\bar{q}}) + \dots \right]}{\sum_q e_q^2 (\sigma_{q\bar{q}} q(x) \bar{q}(x') + \sigma_{qg} q(x) G(x') + \sigma_{gq} G(x) q(x'))}, \quad (120)$$

where the phase space integral $\int \frac{dx}{x} \int \frac{dx'}{x'} \delta(\hat{s} + \hat{t} + \hat{u} - Q^2)$ is implied in both the numerator and denominator. The summation over q includes antiquarks. The dots in (119) and (120) stand for the contributions from the Compton subprocesses, which can be easily deduced from (114). In the small- q_{\perp} region, our definition of $A_{UT}^{\sin(2\phi_{cs} \pm \Phi_S)}$ in terms of the measured cross section (117) agrees with that in [43], but $A_{UT}^{\sin \Phi_S}$ does not because of the different θ_{cs} dependence. We note that the COMPASS Collaboration did not directly confirm the $1 + \cos^2 \theta_{cs}$ dependence of the $\sin \Phi_S$ asymmetry from the data.

The integration over x' can be performed by using the delta function constraint,

$$\delta(\hat{s} + \hat{t} + \hat{u} - Q^2) = \delta \left(-s \left(x' - \frac{m_{\perp} e^{-y}}{\sqrt{s}} \right) \left(x - \frac{m_{\perp} e^y}{\sqrt{s}} \right) + q_{\perp}^2 \right). \quad (121)$$

The minimum of x is attained when $x' = 1$, so the integration range of x is given by

$$1 > x \geq x_{\min} = \frac{m_{\perp} e^y}{\sqrt{s}} + \frac{q_{\perp}^2}{s \left(1 - \frac{m_{\perp} e^{-y}}{\sqrt{s}} \right)}. \quad (122)$$

We also need the following relations in the center-of-mass frame:

$$x_a = \frac{e^y Q^2}{x m_{\perp} \sqrt{s}}, \quad x_b = \frac{Q^2 (x \sqrt{s} - e^y m_{\perp})}{m_{\perp} (x \sqrt{s} m_{\perp} - e^y Q^2)}, \quad c = \frac{Q^2}{q_{\perp}^2 + Q^2}. \quad (123)$$

Alternatively introducing the ‘partonic rapidity’ Y as $x, x' = \sqrt{\frac{\hat{s}}{s}} e^{\pm Y}$, we proceed with

$$\int \frac{dx dx'}{xx'} \delta(\hat{s} + \hat{t} + \hat{u} - Q^2) f(x) g(x') \dots = \int \frac{2dY}{\hat{s} - Q^2} f \left(\sqrt{\frac{\hat{s}}{s}} e^Y \right) g \left(\sqrt{\frac{\hat{s}}{s}} e^{-Y} \right) \dots, \quad (124)$$

where

$$\sqrt{\hat{s}} = m_{\perp} \cosh(Y - y) + \sqrt{m_{\perp}^2 \cosh^2(Y - y) - Q^2}, \quad (125)$$

and

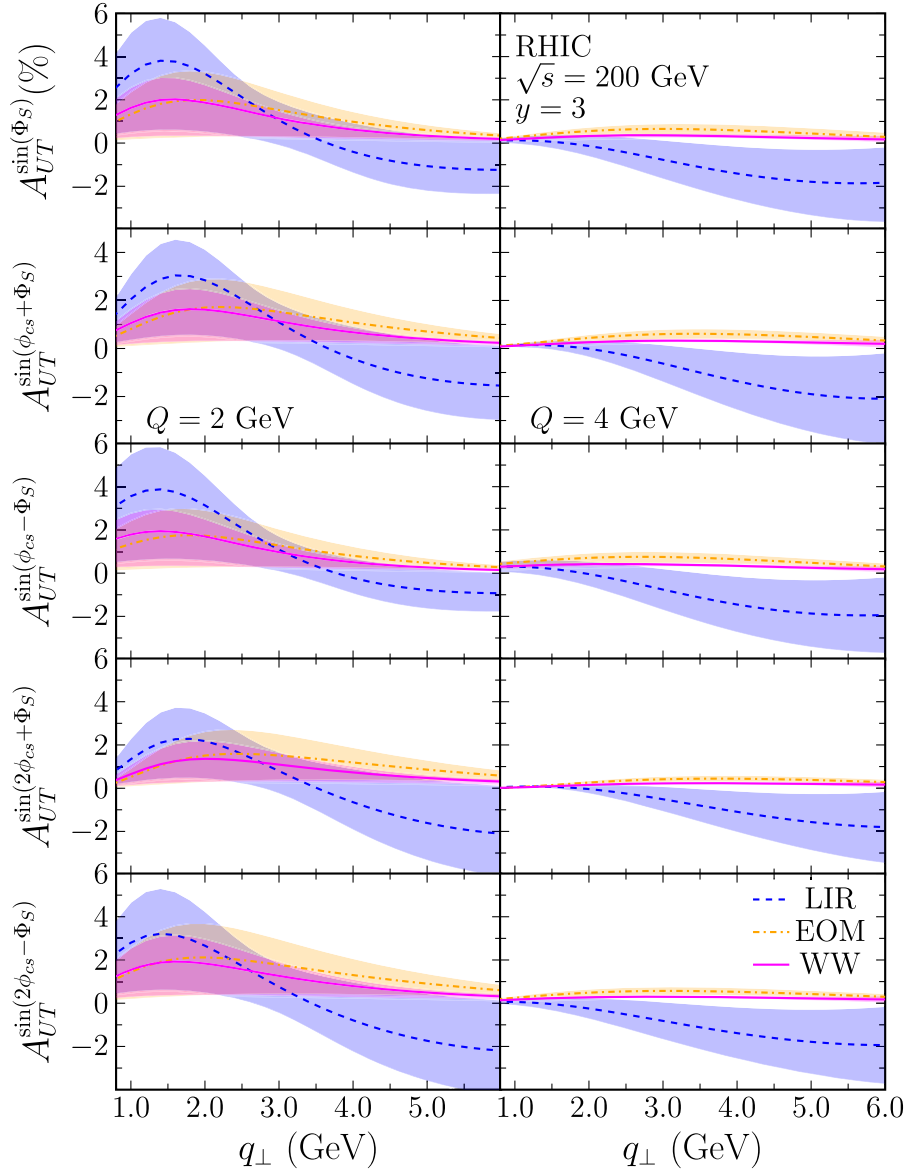


FIG. 7. The q_{\perp} dependencies of all the Drell-Yan asymmetries for the $\sqrt{s} = 200$ GeV RHIC kinematics. Here, we have fixed $y = 3$ and $Q = 2$ GeV (left) and $Q = 4$ GeV (right).

$$x_a = \frac{Q^2}{\sqrt{s}m_{\perp}} e^{y-Y}, \quad x_b = \frac{Q^2}{\sqrt{s}m_{\perp}} e^{Y-y}. \quad (126)$$

We have checked the consistency between the two methods.

The numerical outcomes for the Drell-Yan asymmetries defined by Eqs. (118)–(120) are first given in Fig. 7 for the RHIC kinematics with $\sqrt{s} = 200$ GeV. All the Drell-Yan azimuthal moments are displayed as functions of q_T for the forward case $y = 3$ and with $Q = 2$ GeV (left) and $Q = 4$ GeV (right). When $Q = 2$ GeV, all the considered scenarios, i.e., WW, EOM, and LIR, for $g_T^q(x)$ and $\mathcal{G}_{3T}(x)$, yield percent-level and positive asymmetries in the region $q_T \approx 1\text{--}5$ GeV. The $\sin(\phi_{cs} \pm \Phi_S)$ asymmetries, expected to be small in the TMD framework, are comparable to the

other asymmetries. In the large q_T region, some of the asymmetries tend to be negative in the LIR scenario. While the results are generally largest in magnitude in the LIR scenario, so is the overall uncertainty which is mostly due to scale variations. Interestingly, the results exhibit a strong Q dependence. Shifting to $Q = 4$ GeV, the asymmetries drop to about half of a percent (see a discussion in the concluding section).

In Fig. 8, the RHIC results are presented as functions of the Feynman- x defined by $x_F = 2q^3/\sqrt{s} = 2m_{\perp} \sinh(y)/\sqrt{s}$, so that large and positive x_F corresponds to the forward region, i.e., large x in the polarized proton. Here, we have fixed $Q = 2$ GeV, and $q_{\perp} = 2$ GeV (left) and $q_{\perp} = 5$ GeV (right). x_F can be understood as a proxy

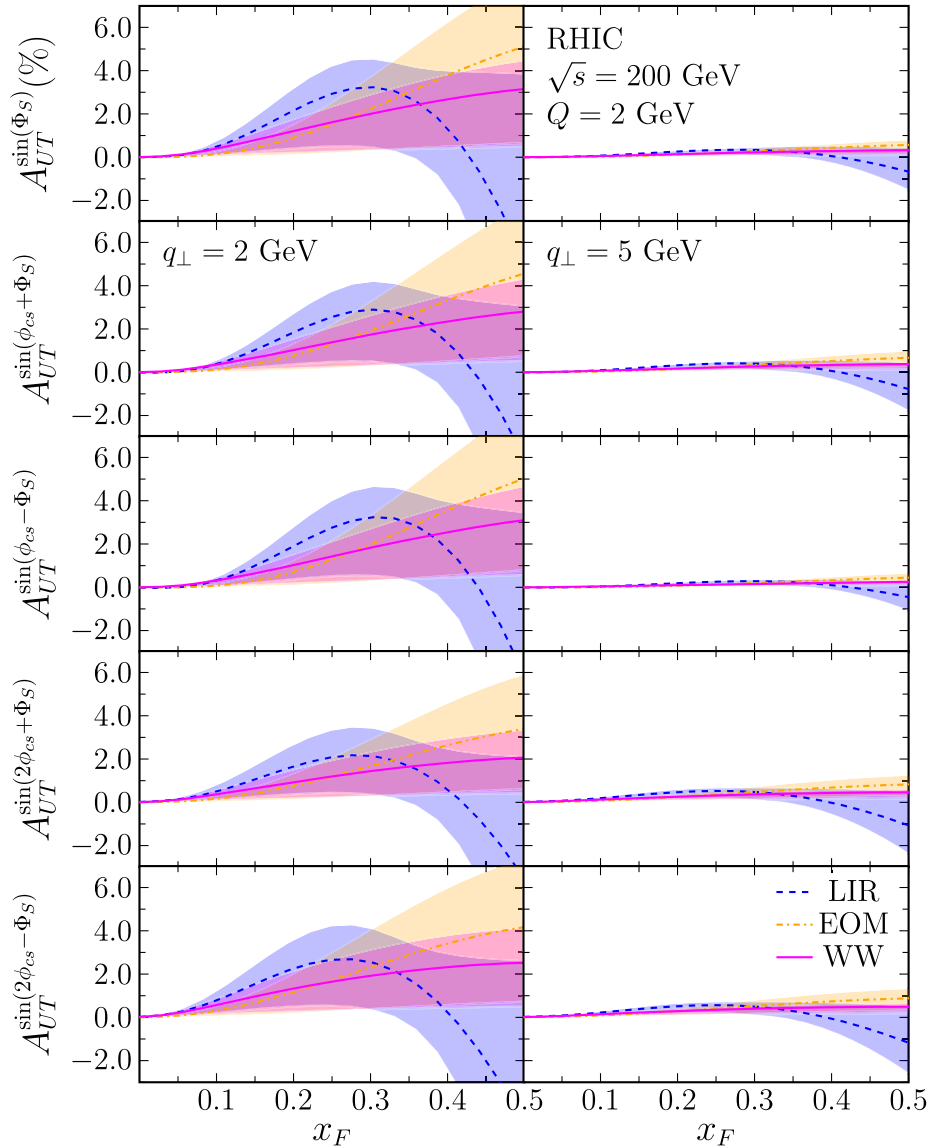


FIG. 8. The x_F dependencies of all the Drell-Yan asymmetries for the $\sqrt{s} = 200$ GeV RHIC kinematics. We have fixed $Q = 2$ GeV and $q_{\perp} = 2(5)$ GeV left (right).

for y with the $x_F = 0.5$ corresponding to the very forward case $y \approx 4.5$. We have also explored the negative x_F region, observing very small, subpercent asymmetries. All the Drell-Yan asymmetries become enhanced in the large x_F region sensitive to the valence content of the polarized proton. For $q_{\perp} = 2$ GeV, the asymmetries are mostly positive, reaching up to about 5% in their central values, with increasing uncertainties. The asymmetries change sign above $x_F \approx 0.4$ in the LIR scenario, reflecting the sign change in the g_T^q PDF and its derivative from Figs. 3 and 4.

Next, we turn to the analysis on the pion induced Drell-Yan process that was measured at COMPASS, where π^- with the momentum 190 GeV collides with a proton at rest [43] corresponding to $\sqrt{s} \approx 18.9$ GeV. We take the

average value of the Drell-Yan virtuality $Q = 5.3$ GeV at COMPASS. Our predictions, shown in Fig. 9 (left), as functions of q_T are obtained by integrating over the rapidity y of the Drell-Yan pair. COMPASS is mostly sensitive to the valence region, so the $\bar{u}u \rightarrow g\gamma$ channel dominates, with the \bar{u} being the valence quark in π^- . The large values of x probed in the polarized proton lead to qualitatively different results for the three scenarios. Whereas in the WW and the EOM scenarios, the asymmetries are positive, and we find mostly negative results in the LIR scenario. COMPASS [43,44] reported $\mathcal{O}(10\%)$ asymmetries for the $\sin \Phi_S$, $\sin(2\phi_{cs} \pm \Phi_S)$ harmonics in the region $q_{\perp} > 1$ GeV, although there are only two data points, and experimental errors are as large as the central values. It is clear that the

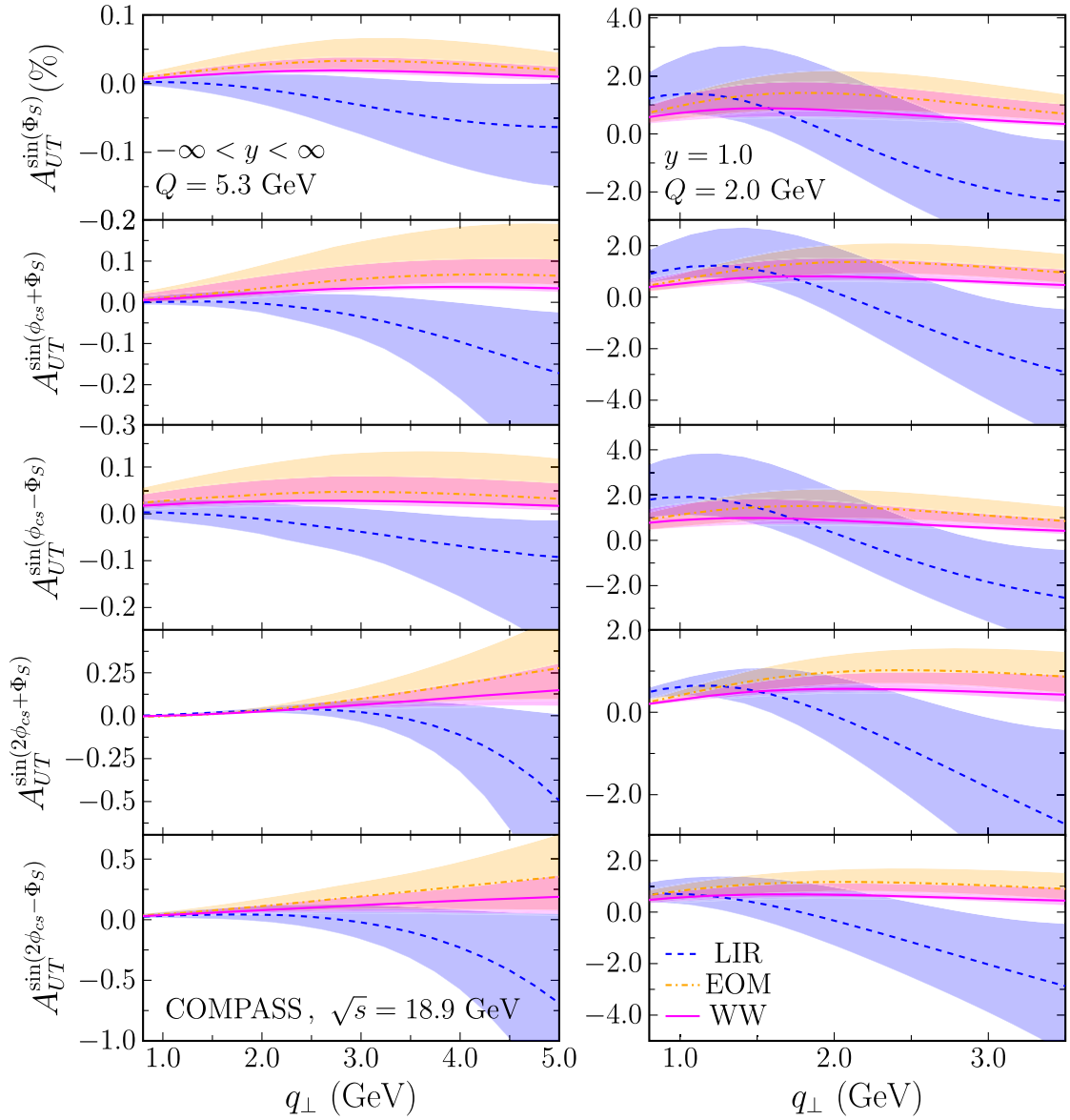


FIG. 9. The asymmetries A_{UT} 's as functions of q_T for the COMPASS kinematics at $\sqrt{s} = 18.9$ GeV. On the left panel, we have fixed $Q = 5.3$ GeV and integrated over the rapidity y of the Drell-Yan pair. On the right panel, the results are obtained for $Q = 2.0$ GeV and $y = 1.0$.

perturbative contribution is very small in the considered kinematics compared to other TMD-based nonperturbative contributions, e.g., [41,45–47]. On the other hand, the asymmetries can reach percent-level magnitude for lower Q values and when large x in the polarized proton is probed, similar to the RHIC case investigated above. This is demonstrated by the right panel of Fig. 9 for $Q = 2$ GeV and $y = 1$, which correspond to $0.24 < x_F < 0.48$ and $1.0 < q_{\perp} < 3.5$ GeV.

Finally, we show in Fig. 10 the predictions for the future fixed target measurement in the SpinQuest experiment at Fermilab [48,49], where a 120 GeV proton (instead of a π^-) collides with a polarized target proton at rest,

corresponding to $\sqrt{s} \approx 15.5$ GeV. On the left panel, we take $Q = 4$ GeV within the intended windows $3 < Q < 10$ GeV and $y = -0.5$, reflecting SpinQuest's preference towards the small- x (sea-quark) regions in the polarized target. With this kinematics, the asymmetries are all subpercent even after the uncertainty bands are taken into account, which increase as q_{\perp} is increased towards the kinematic threshold. On the other hand, when we go to lower Q regions, the perturbative contributions are at the percent level as shown on the right panel in Fig. 10 for $Q = 2$ GeV and $y = 1$. It is seen that the behaviors of various asymmetries are qualitatively similar to the COMPASS π^- results.

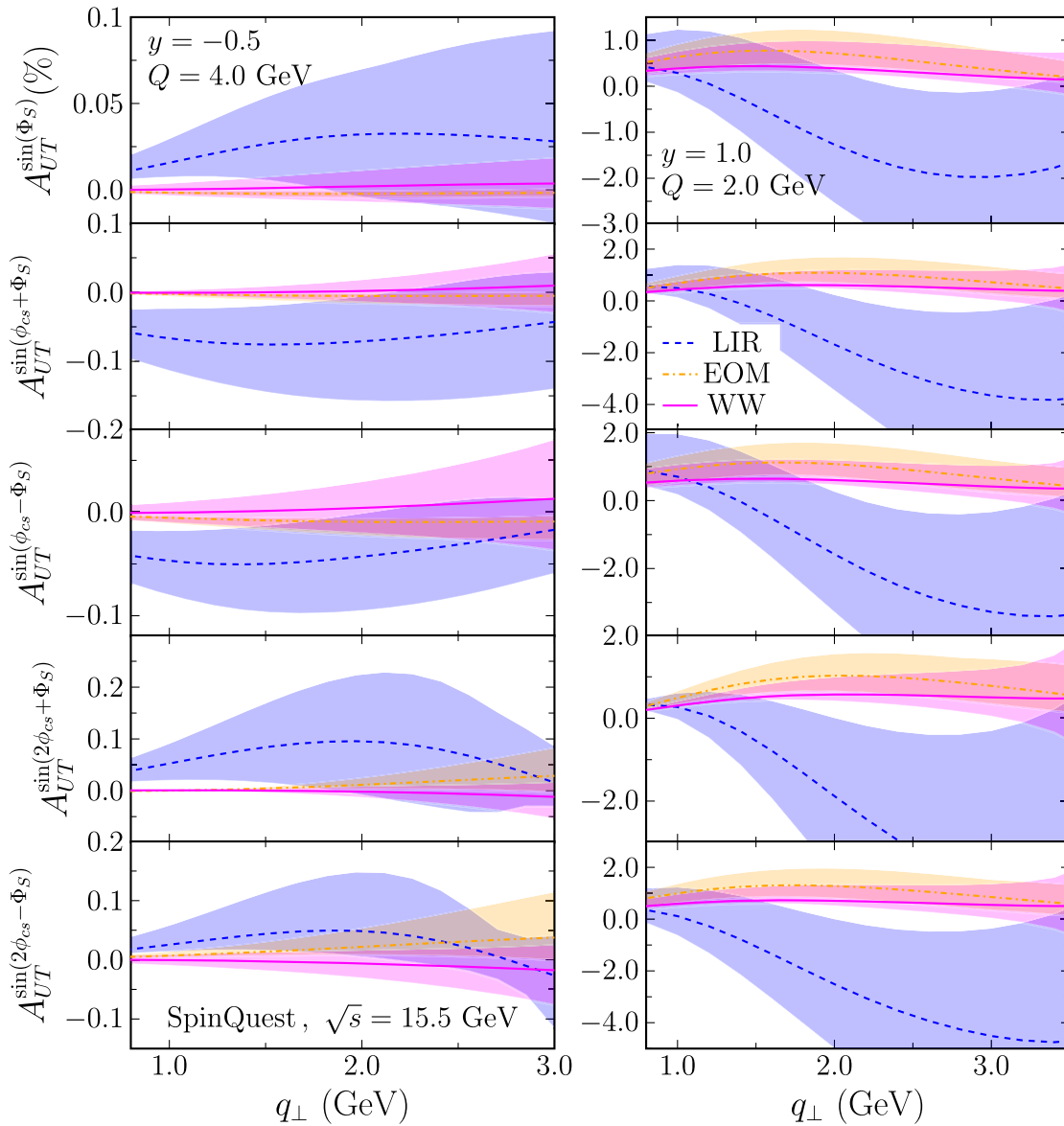


FIG. 10. The asymmetries A_{UT} 's as functions of q_T for the Fermilab SpinQuest collision energy $\sqrt{s} = 15.5$ GeV. We have taken $y = -0.5$, $Q = 4.0$ GeV (left) and $y = 1.0$, $Q = 2.0$ GeV (right).

VI. DISCUSSIONS AND CONCLUSIONS

In this paper, we have proposed a unified formalism to analyze SSAs in SIDIS and the Drell-Yan process and for both longitudinally and transversely polarized protons. The new method is more efficient than our previous brute-force approach to transverse SSAs in SIDIS [2] and actually helps uncover mistakes in part of the earlier calculation [2]. The predictions for transverse SSAs in the Drell-Yan process from the present mechanism are entirely new. We reproduced the known results for the longitudinal polarization case in the literature on both SIDIS [3] and the Drell-Yan process [7,8]. We emphasize that the complete QCD results for SIDIS and the Drell-Yan process have been presented, which should supersede the naive

parton model argument $A_{UT} \sim \alpha_s m_q / \sqrt{s}$ [5] frequently quoted in the literature.

We have observed that the asymmetries in the WW approximation vanish in the limit $Q \rightarrow 0$, i.e., the photo-production limit of SIDIS and direct photon production in pp collisions, and by extension, also in light-hadron production in pp . In these processes and within the WW approximation, SSAs may be indeed proportional to a current quark mass m_q . An evaluation in the parton model with nonzero m_q was performed in [6]. In QCD, the second term in (13) needs to be included, which will cancel the logarithmic singularity $\ln m_q$ in the first term. After this cancellation, we expect a contribution of the form,

$$A_{UT} \propto \alpha_s M_N m_q^2 g_T(x), \quad (127)$$

which is even more suppressed than the naive estimate $A_{UT} \propto \alpha_s m_q$ for light quarks.

Based on the analytical formulas, we have numerically evaluated the asymmetries in the Drell-Yan process relevant to the experiments at RHIC, COMPASS, SpinQuest, and EIC. The asymmetries can reach a few percent level in some preferable kinematics associated with the large- x (valence) region of the polarized proton, but stay at subpercent level elsewhere. Yet, they are one or two orders of magnitude larger than the common prejudice $A_{UT} \sim \mathcal{O}(10^{-4})$ based on the naive estimate $A_{UT} \propto \alpha_s m_q / \sqrt{s}$. The enhancement is mostly attributed to the ratio $M_N / m_q \sim \mathcal{O}(10^2)$, but there is also a suppression factor $x \Delta q(x) / q(x) < 1$ from the PDFs in the WW approximation.

The dependencies of A_{UT} on \sqrt{s} , q_\perp and Q can be roughly inferred from the analytic expressions for the partonic cross sections summarized in Sec. IV F, which, however, will be significantly modified by the convolution with PDFs. In general, there exists no simple analytical formula for $A_{UT}(\sqrt{s}, q_\perp, Q)$. Nevertheless, we have observed that the dependence on \sqrt{s} is relatively weak in the Drell-Yan process, and an approximate power-law behavior in the limit $Q \gg q_\perp$,

$$A_{UT}^{\sin(\alpha\phi_{cs} + \beta\Phi_S)} \propto \left(\frac{q_\perp \text{ or } M_N}{Q} \right)^{B_{\alpha,\beta}}, \quad Q \gg q_\perp, M_N. \quad (128)$$

A numerical extraction gives the exponents,

$$\begin{aligned} B_{0,1} &\sim 1.7, & B_{1,1} &\sim 1.4, & B_{1,-1} &\sim 0.7, \\ B_{2,1} &\sim 0.7, & B_{2,-1} &\sim 1.2, \end{aligned} \quad (129)$$

at $y = 0$ and $q_\perp = 2$. These exponents are sensitive to y (and also to q_\perp to a lesser extent), since dominant partonic channels vary with values of y . In practice, the logarithmic dependence $\ln Q^2 / q_\perp^2$ is also expected in the hard coefficients, which is not taken into account in the above parametrization. We should mention that the scaling (128) is seen only in a region where the magnitude of A_{UT} is already negligibly small. Similarly, in the opposite regime with

$$A_{UT}^{\sin(\alpha\phi_{cs} + \beta\Phi_S)} \propto \left(\frac{Q \text{ or } M_N}{q_\perp} \right)^{C_{\alpha,\beta}}, \quad q_\perp \gg Q, M_N, \quad (130)$$

we find, for $y = 2$ and $Q = 2$,

$$\begin{aligned} C_{0,1} &\sim 2, 0, & C_{1,1} &\sim 1.2, & C_{1,-1} &\sim 1.2, \\ C_{2,1} &\sim 0.8, & C_{2,-1} &\sim 0.8. \end{aligned} \quad (131)$$

These noninteger exponents indicate that the actual q_\perp or Q dependence is more complicated than what naively follows

from the dimensional or twist counting argument $A_{UT} \sim 1/q_\perp$ or $A_{UT} \sim 1/Q$. A similar comment applies to the SIDIS case.

At last, we have also explored the possible impact of the genuine twist-three corrections using the recent extraction of $g_T(x)$ from the global analysis [9] and the equations of motion [10]. It was found that these corrections tend to enhance the asymmetries and can even flip the sign of the asymmetries in the LIR scenario. However, since our formulas involve the derivative of $g_T(x)$, uncertainties of $g_T(x)$ are amplified. A more accurate determination of $g_T(x)$ is therefore welcome for future studies.

ACKNOWLEDGMENTS

We thank Shohini Bhattacharya, Genki Nukazuka, Marc Schlegel, Werner Vogelsang, Shinsuke Yoshida, and Feng Yuan for discussions and correspondences. The work of S.B. and A.K. is supported by the Croatian Science Foundation (HRZZ) Grant No. 5332 (UIP-2019-04). Y.H. is supported by the U.S. Department of Energy under Contract No. DE-SC0012704, and also by Laboratory Directed Research and Development (LDRD) funds from Brookhaven Science Associates. H.-n. L. is supported by National Science and Technology Council of the Republic of China under Grant No. MOST-110-2112-M-001-026-MY3. S.B. is thankful for the warm hospitality at the University of Tübingen in 2022, where part of this work was done.

APPENDIX: COMPUTATION OF THE HARD KERNEL IN SIDIS

In this Appendix, we outline the main steps to arrive at (21). Starting from (34) of [2], we write

$$\begin{aligned} \mathcal{H}_{\mu\nu}(p) T_r^{\mu\nu} &= -\frac{2\pi i g^4}{N_c} \\ &\times \int \frac{d^4 l_2}{(2\pi)^4} (2\pi) \delta(l_2^2) (2\pi) \delta((p+q-l_2)^2) W_r, \end{aligned} \quad (A1)$$

where

$$\begin{aligned} W_r &\equiv T_{r,\mu\nu} \text{Tr}[\gamma_5 \not{p} A^{\alpha\mu}(p+q-p_q) \\ &\times \bar{M}_{\alpha\beta}(p+q-p_q, l_2) A^{\nu\beta}(l_2)]. \end{aligned} \quad (A2)$$

The building blocks \bar{M} and A were introduced in [2], which are given by

$$\bar{M}_{\alpha\beta} = \sum_{l=1}^3 c_l \frac{m_{l,\alpha\beta}}{d_l}, \quad (A3)$$

$$\begin{aligned}
c_1 &= \frac{N_c(N_c^2 - 1)}{4}, & m_{1,\alpha\beta} &= -V_{\alpha\beta\rho}(p + q - p_q, l_2) \not{p}_q \gamma^\rho (\not{p} + \not{q} - \not{l}_2), & d_1 &= (p + q - p_q - l_2)^2, \\
c_2 &= \frac{(N_c^2 - 1)^2}{4N_c}, & m_{2,\alpha\beta} &= \not{p}_q \gamma_\alpha (\not{p} + \not{q}) \gamma_\beta (\not{p} + \not{q} - \not{l}_2), & d_2 &= (p + q)^2, \\
c_3 &= \frac{N_c^2 - 1}{4N_c}, & m_{3,\alpha\beta} &= -\not{p}_q \gamma_\beta (\not{p}_q - \not{l}_2) \gamma_\alpha (\not{p} + \not{q} - \not{l}_2), & d_3 &= (p_q - l_2)^2,
\end{aligned} \tag{A4}$$

with V being the three-gluon vertex, and

$$\begin{aligned}
A^{\alpha\mu} &= \sum_{i=1}^2 \frac{a_{Li}^{\alpha\mu}}{d_{Lj}}, & a_{L1}^{\alpha\mu} &= \gamma^\alpha (\not{p}_q - \not{q}) \gamma^\mu, & a_{L2}^{\alpha\mu} &= \gamma^\mu (\not{p} + \not{q}) \gamma^\alpha, & d_{L1} &= (p_q - q)^2, & d_{L2} &= (p + q)^2, \\
A^{\nu\beta} &= \sum_{j=1}^2 \frac{a_{Rj}^{\nu\beta}}{d_{Rj}}, & a_{R1}^{\nu\beta} &= \gamma^\nu (\not{p} - \not{l}_2) \gamma^\beta, & a_{R2}^{\nu\beta} &= \gamma^\beta (\not{p} + \not{q}) \gamma^\nu, & d_{R1} &= (p - l_2)^2, & d_{R2} &= (p + q)^2.
\end{aligned} \tag{A5}$$

We perform the loop integral as

$$\int \frac{d^4 l_2}{(2\pi)^4} (2\pi) \delta(l_2^2) (2\pi) \delta((p + q - l_2)^2) = \frac{1}{32\pi^2} \sum_{a_2=\pm} \int_0^1 d\Delta_2 \int_0^{2\pi} d\phi_2, \tag{A6}$$

where $l_{2(a_2)}^\pm$ denote the solutions of the δ -function conditions $l_2^2 = 0$ and $(p + q - l_2)^2 = 0$, namely,

$$l_{2(a_2)}^+ = \frac{p^+ + q^+}{2} (1 + a_2 \Delta_2), \quad l_{2(a_2)}^- = \frac{q^-}{2} (1 - a_2 \Delta_2), \quad \Delta_2 = \sqrt{1 - \frac{4l_{2\perp}^2}{s}}, \quad a_2 = \pm 1. \tag{A7}$$

In addition, we also have the on-shell conditions for the tagged parton $p_q^2 = 0$ and $(p + q - p_q)^2 = 0$, that produce

$$p_{q(a_q)}^+ = \frac{p^+ + q^+}{2} (1 + a_q \Delta_q), \quad p_{q(a_q)}^- = \frac{q^-}{2} (1 - a_q \Delta_q), \quad \Delta_q = \sqrt{1 - \frac{4p_{q\perp}^2}{s}}, \quad a_q = \pm 1. \tag{A8}$$

Next, we write the Dirac trace as

$$W_r = \sum_{ij=1}^2 \sum_{l=1}^3 c_l \frac{W_{r,ilj}}{d_{Li} d_l d_{Rj}}, \tag{A9}$$

where

$$W_{r,ilj} = T_{r,\mu\nu} \text{Tr} \left[\gamma_5 \not{k} a_{Li}^{\alpha\mu} m_{l,\alpha\beta} a_{Rj}^{\nu\beta} \right], \tag{A10}$$

and d_l in the denominator contains the ϕ_2 angular dependence. After the computation of the Dirac traces, the angular dependence in the numerator takes the form,

$$W_{r,ilj} = \sum_{g=0}^3 w_{r,ilj}^{(g)} \left(\frac{p_{q\perp} \cdot l_{2\perp}}{s} \right)^g. \tag{A11}$$

The ϕ_2 integral can then be performed analytically, leading to

$$\int_0^{2\pi} d\phi_2 \frac{1}{d_l} \left(\frac{p_{q\perp} \cdot l_{2\perp}}{s} \right)^g = \frac{2\pi}{s} I_{g,l}, \tag{A12}$$

where

$$\begin{aligned}
I_{0,1}^{(a_q, a_2)} &= -\frac{2}{|a_q \Delta_q + a_2 \Delta_2|}, \\
I_{1,1}^{(a_q, a_2)} &= -\frac{1}{2} \left(1 - \frac{1 + a_q a_2 \Delta_q \Delta_2}{|a_q \Delta_q + a_2 \Delta_2|} \right), \\
I_{2,1}^{(a_q, a_2)} &= \frac{1}{8} (1 + a_q a_2 \Delta_q \Delta_2) \left(1 - \frac{1 + a_q a_2 \Delta_q \Delta_2}{|a_q \Delta_q + a_2 \Delta_2|} \right), \\
I_{3,1}^{(a_q, a_2)} &= -\frac{1}{32} (1 - \Delta_q^2)(1 - \Delta_2^2) \left[\frac{1}{2} + \frac{(1 + a_q a_2 \Delta_q \Delta_2)^2}{(1 - \Delta_q^2)(1 - \Delta_2^2)} \left(1 - \frac{1 + a_q a_2 \Delta_q \Delta_2}{|a_q \Delta_q + a_2 \Delta_2|} \right) \right], \\
I_{0,2}^{(a_q, a_2)} &= 1, \\
I_{1,2}^{(a_q, a_2)} &= 0, \\
I_{2,2}^{(a_q, a_2)} &= \frac{1}{32} (1 - \Delta_q^2)(1 - \Delta_2^2), \\
I_{3,2}^{(a_q, a_2)} &= 0, \\
I_{0,3}^{(a_q, a_2)} &= -\frac{2}{|a_q \Delta_q - a_2 \Delta_2|}, \\
I_{1,3}^{(a_q, a_2)} &= \frac{1}{2} \left(1 - \frac{1 - a_q a_2 \Delta_q \Delta_2}{|a_q \Delta_q - a_2 \Delta_2|} \right), \\
I_{2,3}^{(a_q, a_2)} &= \frac{1}{8} (1 - a_q a_2 \Delta_q \Delta_2) \left(1 - \frac{1 - a_q a_2 \Delta_q \Delta_2}{|a_q \Delta_q - a_2 \Delta_2|} \right), \\
I_{3,3}^{(a_q, a_2)} &= \frac{1}{32} (1 - \Delta_q^2)(1 - \Delta_2^2) \left[\frac{1}{2} + \frac{(1 - a_q a_2 \Delta_q \Delta_2)^2}{(1 - \Delta_q^2)(1 - \Delta_2^2)} \left(1 - \frac{1 - a_q a_2 \Delta_q \Delta_2}{|a_q \Delta_q - a_2 \Delta_2|} \right) \right]. \tag{A13}
\end{aligned}$$

The above relations allow us to get

$$\mathcal{H}(p) \cdot T_r = -\frac{ig^4}{8N_c s} \sum_{a_2=\pm} \int_0^1 d\Delta_2 \sum_{ijl} \frac{1}{d_{Li} d_{Rj}} \sum_g w_{r,ijl}^{(g)(a_q, a_2)} I_{g,l}^{(a_q, a_2)}, \tag{A14}$$

with

$$\Delta_q = a_q \left(1 + \frac{2t}{s + Q^2} \right). \tag{A15}$$

Because there is no collinear divergence in the sum over $ijlg$, the Δ_2 integral can be safely done. The result is actually independent of a_2 , so the summation over a_2 simply gives a factor of 2. It is then straightforward to derive (21).

-
- | | |
|--|--|
| <p>[1] S. Benic, Y. Hatta, H.-n. Li, and D.-J. Yang, <i>Phys. Rev. D</i> 100, 094027 (2019).</p> <p>[2] S. Benić, Y. Hatta, A. Kaushik, and H.-n. Li, <i>Phys. Rev. D</i> 104, 094027 (2021).</p> <p>[3] M. Abele, M. Aicher, F. Piacenza, A. Schäfer, and W. Vogelsang, <i>Phys. Rev. D</i> 106, 014020 (2022).</p> <p>[4] R. Boughezal, D. de Florian, F. Petriello, and W. Vogelsang, <i>Phys. Rev. D</i> 107, 075028 (2023).</p> | <p>[5] G. L. Kane, J. Pumplin, and W. Repko, <i>Phys. Rev. Lett.</i> 41, 1689 (1978).</p> <p>[6] W. G. D. Dharmaratna and G. R. Goldstein, <i>Phys. Rev. D</i> 53, 1073 (1996).</p> <p>[7] R. D. Carlitz and R. S. Willey, <i>Phys. Rev. D</i> 45, 2323 (1992).</p> <p>[8] H. Yokoya, <i>Prog. Theor. Phys.</i> 118, 371 (2007).</p> <p>[9] S. Bhattacharya, Z.-B. Kang, A. Metz, G. Penn, and D. Pitonyak, <i>Phys. Rev. D</i> 105, 034007 (2022).</p> |
|--|--|

- [10] B. Bauer, D. Pitonyak, and C. Shay, *Phys. Rev. D* **107**, 014013 (2023).
- [11] R.-b. Meng, F. I. Olness, and D. E. Soper, *Nucl. Phys.* **B371**, 79 (1992).
- [12] P. G. Ratcliffe, *Nucl. Phys.* **B264**, 493 (1986).
- [13] A. V. Efremov and O. V. Teryaev, *Phys. Lett.* **150B**, 383 (1985).
- [14] J.-w. Qiu and G. F. Sterman, *Phys. Rev. Lett.* **67**, 2264 (1991).
- [15] H. Eguchi, Y. Koike, and K. Tanaka, *Nucl. Phys.* **B763**, 198 (2007).
- [16] Y. Koike and S. Yoshida, *Phys. Rev. D* **85**, 034030 (2012).
- [17] S. Yoshida, *Phys. Rev. D* **93**, 054048 (2016).
- [18] A. Metz, M. Schlegel, and K. Goeke, *Phys. Lett. B* **643**, 319 (2006).
- [19] Y. V. Kovchegov and M. D. Sievert, *Phys. Rev. D* **86**, 034028 (2012); **86**, 079906(E) (2012).
- [20] M. Schlegel, *Phys. Rev. D* **87**, 034006 (2013).
- [21] S. Benić, D. Horvatić, A. Kaushik, and E. A. Vivoda, *Phys. Rev. D* **106**, 114025 (2022).
- [22] H. Xing and S. Yoshida, *Phys. Rev. D* **100**, 054024 (2019).
- [23] X.-D. Ji, *Phys. Lett. B* **289**, 137 (1992).
- [24] Y. Hatta, K. Tanaka, and S. Yoshida, *J. High Energy Phys.* **02** (2013) 003.
- [25] J. C. Collins and D. E. Soper, *Phys. Rev. D* **16**, 2219 (1977).
- [26] R. D. Tangerman and P. J. Mulders, *Phys. Rev. D* **51**, 3357 (1995).
- [27] S. Arnold, A. Metz, and M. Schlegel, *Phys. Rev. D* **79**, 034005 (2009).
- [28] M. Boglione and S. Melis, *Phys. Rev. D* **84**, 034038 (2011).
- [29] X. Ji, J.-w. Qiu, W. Vogelsang, and F. Yuan, *Phys. Rev. D* **73**, 094017 (2006).
- [30] J. Zhou and A. Metz, *Phys. Rev. D* **86**, 014001 (2012).
- [31] B. Pire and J. P. Ralston, *Phys. Rev. D* **28**, 260 (1983).
- [32] H. H. Patel, *Comput. Phys. Commun.* **197**, 276 (2015).
- [33] J. G. Korner, B. Melic, and Z. Merebashvili, *Phys. Rev. D* **62**, 096011 (2000).
- [34] J. G. Korner and G. Schuler, *Z. Phys. C* **26**, 559 (1985).
- [35] K. Hagiwara, K.-i. Hikasa, and N. Kai, *Phys. Rev. Lett.* **52**, 1076 (1984).
- [36] K. Hagiwara, K.-i. Hikasa, and N. Kai, *Phys. Rev. D* **27**, 84 (1983).
- [37] M. G. Santiago, *Phys. Rev. D* **109**, 034004 (2024).
- [38] J. J. Ethier, N. Sato, and W. Melnitchouk, *Phys. Rev. Lett.* **119**, 132001 (2017).
- [39] J. F. Owens, A. Accardi, and W. Melnitchouk, *Phys. Rev. D* **87**, 094012 (2013).
- [40] H.-L. Lai, M. Guzzi, J. Huston, Z. Li, P. M. Nadolsky, J. Pumplin, and C. P. Yuan, *Phys. Rev. D* **82**, 074024 (2010).
- [41] J. Cammarota, L. Gamberg, Z.-B. Kang, J. A. Miller, D. Pitonyak, A. Prokudin, T. C. Rogers, and N. Sato (Jefferson Lab Angular Momentum Collaboration), *Phys. Rev. D* **102**, 054002 (2020).
- [42] P. C. Barry, C.-R. Ji, N. Sato, and W. Melnitchouk (Jefferson Lab Angular Momentum (JAM) Collaboration), *Phys. Rev. Lett.* **127**, 232001 (2021).
- [43] M. Aghasyan *et al.* (COMPASS Collaboration), *Phys. Rev. Lett.* **119**, 112002 (2017).
- [44] G. D. Alexeev *et al.* (COMPASS Collaboration), arXiv: 2312.17379.
- [45] M. G. Echevarria, Z.-B. Kang, and J. Terry, *J. High Energy Phys.* **01** (2021) 126.
- [46] M. Bury, A. Prokudin, and A. Vladimirov, *J. High Energy Phys.* **05** (2021) 151.
- [47] B. Gurjar and C. Mondal, *Phys. Rev. D* **109**, 014038 (2024).
- [48] C. Brown *et al.*, 10.2172/1296770 (2014).
- [49] A. Chen *et al.* (SeaQuest Collaboration), *Proc. Sci.*, SPIN2018 (2019) 164 [arXiv:1901.09994].